Joint Deployment and Resource Management for VLC-enabled RISs-assisted UAV Networks

Yihan Cang, *Student Member, IEEE*, Ming Chen, *Member, IEEE*,
Jingwen Zhao, *Student Member, IEEE*, Zhaohui Yang, *Member, IEEE*,
Ye Hu, *Member, IEEE*, Chongwen Huang, *Member, IEEE*,
Kai-Kit Wong, *Fellow, IEEE*

***Abstract*—In this paper, the problem of the deployment and resource management for visible light communication (VLC)-enabled, reconfigurable intelligent surfaces (RISs)-assisted unmanned aerial vehicle (UAV) networks is investigated. In the considered model, UAVs provide terrestrial users with wireless services and illumination simultaneously. Moreover, RISs are utilized to further improve the channel quality between UAVs and users. This joint placement and resource management problem is constructed aiming at acquiring the optimal UAV deployment, RISs phase shift, user and RIS association that satisfies the users' needs with minimum consumption of the UAVs' energy. An iterative algorithm that alternately optimizes continuous and binary variables is proposed to solve this mixed-integer programming problem. Specifically, RISs phase shift optimization is solved by phases alignment method and semidefinite program algorithm. Next, the successive convex approximation algorithm is proposed to settle the UAV deployment problem. The user and RIS association variables are relaxed to the continuous ones before adopting the dual method to find the optimal solution. Moreover, a greedy algorithm is proposed as an alternative to RIS association optimization with low complexity. Simulation results show that the proposed two schemes harvest the superior performance of 34.85% and 32.11% energy consumption reduction over the case without RIS, respectively.**

***Index Terms*—Visible light communication, unmanned aerial vehicles, reconfigurable intelligent surfaces, energy efficiency.**

I. Introduction

Nowadays, mobile applications such as mobile health computing, mobile object recognition and extended reality are emerging with the development of novel science and technology such as visible light communication (VLC) [1] and unmanned aerial vehicle (UAV) [2]–[5]. Their requirements for extremely high data rate, high quality-of-service (QoS), and ultra-low latency are driving the revolution of mobile wireless networks [6]–[8]. Fortunately, the reconfigurable intelligent surfaces (RISs), or intelligent reflecting surfaces (IRSs), can improve spectrum and energy efficiency in wireless systems [9]–[11] by reflecting the signals without any signal processing operations [12]. Phase shift needs to be elaborately optimized on RIS for a certain communication purpose. However, problems of phase shift optimization is particular challenging in considered UAV communication systems, since the phase shift of RIS has relations with the UAV placement as well.

Recently, a number of existing literature such as [13]–[28] have focused on the use of RISs in wireless communication. The maximum weighted sum-rate in RIS-assisted multi-cell networks was investigated in [13]. The coverage of a downlink RIS-aided network that consists of one base station (BS) and a single user was analyzed and maximized in [14]. The work in [15] optimized the resource allocation in a network that consists of a RIS-assisted wireless transmitter and multiple receivers. The joint design of transmit beamforming matrix at the base station and the phase shift matrix at the RIS was studied in [16], by utilizing deep reinforcement learning (DRL). The property of RIS-assisted nonorthogonal-multiple-access (NOMA) system has been analyzed in [17]–[21]. The aforementioned works in [13]–[23] studied the applications of RISs in radio frequency (RF) communication. Meanwhile, the works [24] and [24]–[28] studied the applications of RISs in terahertz (THz) band and millimeter wave band, respectively. However, none of these existing works including [13]–[28] studied the use of RISs for VLC system.

Thanks to the advantage of tremendous bandwidth, VLC is a promising paradigm to remedy the problem of spectrum resource shortage in the next generation wireless networks [29]–[31]. Besides, VLC has other advantages over RF with regards to excellent energy efficiency, no health hazards and so on [32], [33]. Moreover, compared with RIS-aided RF, RIS-aided VLC can provide communications and illumination simultaneously. However, the transmitted signals shall be real and non-negative in VLC, thus the signal process in VLC is far different from that in RF. Therefore, the aforementioned conventional methods in RIS-aided RF [13]–[15], [17]–[28] can not be directly employed in VLC due to its unique characteristics.

It is well known that VLC is usually applicable to indoor scenarios. Nevertheless, one can use UAVs to offer both communications and illumination to terrestrial users in order to

This work was supported in part by the National Key Research and Development Program under grant 2018YFB1801905, by the National Natural Science Foundation of China (NSFC) under grant 61960206005 & 61960206006. *(Corresponding author: Ming Chen.)*

Y. Cang, M. Chen and J. Zhao are with the National Mobile Communications Research Laboratory, Southeast University, Nanjing 210096, China (e-mails: yhcang@seu.edu.cn, chenming@seu.edu.cn, zhaojingwen@seu.edu.cn). M. Chen is also with the Purple Mountain Laboratories, Nanjing 211100, China.

Z. Yang is with College of Information Science and Electronic Engineering Zhejiang Key Lab of Information Processing Communication and Networking, Zhejiang University, and also with the Department of Electronic and Electrical Engineering, University College London, UK. (e-mail: zhaohui.yang@ucl.ac.uk).

Y. Hu is with the Department of Electrical Engineering, Columbia University, NewYork, NY, 10027, USA (e-mail: yh3453@columbia.edu).

C. Huang is with College of Information Science and Electronic Engineering, Zhejiang University, Hangzhou 310027, China, and with International Joint Innovation Center, Zhejiang University, Haining 314400, China, and also with Zhejiang Provincial Key Laboratory of Info. Proc., Commun. & Netw. (IPCAN), Hangzhou 310027, China (e-mail: chongwenhuang@zju.edu.cn).

K. Wong is with the Department of Electronic and Electrical Engineering, University College London, London, UK (e-mail: kai-kit.wong@ucl.ac.uk).

enable VLC to be utilized in outdoor scenarios since UAVs can fly to proximity of users [4], [5]. In fact, deploying UAVs as flying BSs for wireless networks is a flexible and cost-effective approach to providing on-demand communications. However, for tomorrow's ultra dense wireless networks, UAVs deployed as aerial BSs using RF will interfere with ground devices thus significantly affecting the performance of the ground network. In addition, the limited energy will restrict the applicability of UAVs using RF resource to provide high-speed communication services for ground users. These challenges can be addressed by equipping UAVs with VLC capabilities. Indeed, a VLC system that uses light-emitting diodes (LEDs) to transmit wireless signals can provide both illumination and communication services. Moreover, the altitude of the UAVs increases the probability of LoS channel for VLC. Therefore, using VLC can be a promising approach to provide energy-efficient UAV communications with sufficiently available bandwidth for use cases, such as midnight in the disaster area. A lot of existing works has studied the problems related VLC-enabled UAVs. Particularly, in [34] the power consumption of VLC-enabled UAVs that must provide communications and illumination is optimized. Authors in [35] utilized machine learning (ML) technology to predict the illumination requirements of users for purpose of optimizing the deployment of the VLC-enabled UAVs. The use of NOMA techniques for VLC-enabled UAVs to achieve the maximum sum rate of users was investigated in [36]. However, the optical wireless channel (OWC) consists of Line-of-Sight (LoS) channel, which represents the rectilinear propagation between transmitter and receiver, and Non-Line-of-Sight (NLoS) channel, which fades severely during the propagation via reflection, scattering and so on [37], [38]. In outdoor scenario, there exists a lot of obstacles such as buildings, large billboard and even trees. With the help of RIS, a UAV-RIS-user link which consists of two LoS sublinks can be constructed even there exists obstacles between UAV and terrestrial users.

Motivated by this, a novel framework that enables the UAVs to jointly use RISs and VLC to serve terrestrial users in regards to energy efficiency is proposed in this paper. The key contributions are listed as follows:

- We propose a novel VLC-enabled, RISs-assisted UAV communication system to achieve higher energy efficiency. Within this system, UAVs offer wireless services and illumination simultaneously to terrestrial users. Multiple RISs are deployed to construct additional RISs-reflecting links. With the help of RISs, the channels quality between UAVs and terrestrial users is improved, and thus higher energy efficiency is achieved.
- To coordinate the operations on UAVs and RISs for optimal energy efficiency, the problem of joint placement and resource management is studied. In particular, this problem is constructed as an optimization framework aiming to acquire the optimal UAV deployment, RIS phase shift, user and RIS association, while the constraints of traffic rate and illumination requirements need to be satisfied.
- A novel, low-complexity algorithm that alternately optimizes UAV deployment, phase shifts of RISs, user and RIS association is proposed. In particular, first, the optimizations of RISs phase shift in two application scenarios are solved by phases alignment method and semidefinite program (SDP) algorithm, respectively. Then, the non-convex UAV deployment problem is transformed into a series of convex subproblems through successive convex approximation (SCA) method. Besides, the user and RIS association problem is solved by using relaxation and dual techniques. Finally, we propose a greedy algorithm as an alternative to RIS association optimization with low complexity.

Simulation results show that the gaps between the proposed schemes and the global optimal scheme are small, which indicates that the proposed schemes approach the optimal solution. Besides, our proposed two schemes can yield 34.85% and 32.11% energy consumption reduction over the case without RIS, respectively, which shows that RIS can effectively enhance the channel gains between UAVs and users. From simulations, we can also find that the optimal locations of UAVs are surrounded by its associated users and RISs. Furthermore, a small number of users who are distant from most users are served by an individual UAV, which can reduce the total transmit power significantly. Moreover, each RIS is associated with the closest UAV among all UAVs due to the short distance between UAV and RIS can enhance the channel gains between UAV and terrestrial users, thus reducing the transmit power.

The rest of this paper is structured as follows. Section II elaborates the system model and problem formulation. The proposed algorithms that alternately optimize UAV deployment, phase shifts of RISs, user and RIS association are rendered in Section III. Simulation results are represented in Section IV. Section V draws the conclusions.

II. System Model and Problem Formulation

Consider a geographical area $\mathcal{A}$ where a set $\mathcal{U}$ of U terrestrial users need downlink data and illumination service. A VLC-enabled UAV network which includes a set $\mathcal{D}$ of D UAVs, and a set $\mathcal{L}$ of L RISs is deployed to serve such service needs, as shown in Fig. 1. In this network, each UAV can provide terrestrial users with communication and illumination simultaneously.[1] For communication service, each UAV can directly transmit the data to the requested terrestrial users or it can transmit the data to RISs that will reflect the data to the terrestrial users. Assume that each UAV can only serve terrestrial users until it flies into the view (communication range) of the target users.[2] Thereinafter, we use aerial area

[1]Note that the considered model is especially applicable to some emergency scenarios, such as disaster relief scenes.

[2]The differences between UAVs and ground base stations lie in mainly two aspects. Firstly, the location of ground base station is usually fixed once it is deployed. However, UAVs can be flexibly deployed due to their unique flying characteristics. Secondly, conventional base stations are usually deployed on the ground while UAVs can fly on the air to provide service for users. This results in the difference of the channels between UAV networks and convention ground networks as the probability of LoS links in UAV network is much higher than that in ground networks. Therefore, UAVs is more suitable to the dynamic scenarios with user mobility and emergency scenarios.

This article has been accepted for publication in a future issue of this journal, but has not been fully edited. Content may change prior to final publication. Citation information: DOI 10.1109/TWC.2022.3165853, IEEE Transactions on Wireless Communications

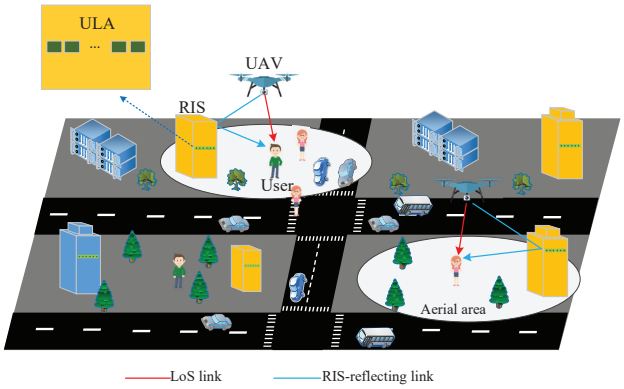

Fig. 1: The architecture of VLC-enabled UAV multi-cell networks with RISs assisted.

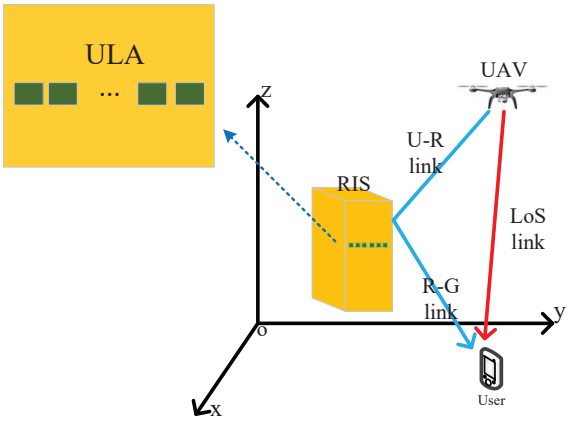

Fig. 2: An RIS-assisted VLC communication system.

to represent the area that falls within the service coverage of one UAV. Moreover, in our network, the rotary-wing UAV is considered. The UAVs will, with a steady speed, travel across the aerial area in a steady straight-and-level flight (SLF), and, then, hover over the aerial area with a steady circular flight (SCF) to to serve the users. Thus, the UAVs can be regarded as static aerial base stations during wireless transmission.[3]

A. Transmission Model

The location of ground user $j \in \mathcal{U}$ is denoted by $(v_j, w_j, 0) \in \mathcal{A}$. And the location of UAV $i \in \mathcal{D}$ is denoted by (x_i, y_i, H), in which H is the altitude of each UAV and is assumed to be identical and fixed for all UAVs. As shown in Fig. 2, the RISs are deployed on the buildings. The location of RIS l is denoted by (a_l, b_l, z_R). Without loss of generality, the height of all RISs is assumed to be the same. We consider the user association among multiple UAVs and users. Specifically, denote u_{ij} as the association between UAV i and ground user j. If $u_{ij} = 1$, ground user j is served by UAV i; otherwise, $u_{ij} = 0$. Since each ground user can be served by only one UAV, we have the following equation

$$\sum_{i \in \mathcal{D}} u_{ij} = 1, \quad \forall j \in \mathcal{U}. \tag{1}$$

In our model, we consider two types of data transmission links: 1) UAV-users, i.e., the direct line of sight (LoS) link; 2) UAV-RIS-users, i.e., RIS-reflecting link.

1) Direct LoS link channel model: The direct LoS link channel gain between UAV i and user j can be expressed by

$$h_{ij}^{LoS} = \begin{cases} \frac{(k+1)A}{2\pi d_{ij}^2} \cos^k(\phi_{ij}) g(\varphi_{ij}) \cos(\varphi_{ij}), & 0 \le \varphi_{ij} \le \Psi_c, \\ 0, & \varphi_{ij} > \Psi_c, \end{cases} \tag{2}$$

where $k = -\frac{\ln 2}{\ln \cos(\Phi_{\frac{1}{2}})}$ denotes the Lambertian emission order with $\Phi_{\frac{1}{2}}$ being the semi angle at half-power of the transmitter. A represents the physical area of the PD in each receiver and d_{ij} represents the distance between UAV i and ground user j. In (2), the light emission and incidence angle from UAV i to ground user j are represented by ϕ_{ij} and φ_{ij}, respectively. Besides, $\Psi_c \le \pi/2$ denotes the receiver's field of view, and the gain of the optical concentrator $g(\varphi_{ij})$ is defined as

$$g(\varphi_{ij}) = \begin{cases} \frac{n^2}{\sin^2(\Psi_c)}, & 0 \le \varphi_{ij} \le \Psi_c, \\ 0, & \varphi_{ij} > \Psi_c, \end{cases} \tag{3}$$

where n denotes internal reflective index.

2) RIS-reflecting link channel model: For tractability, let m_{il} denote the association chance between UAV i and RIS l, such that if RIS l is in the aerial area of UAV i, we have $m_{il} = 1$; otherwise, $m_{il} = 0$. Since each RIS can be located in only one UAV's aerial area, then we have the following equation

$$\sum_{i \in \mathcal{D}} m_{il} = 1, \quad \forall l \in \mathcal{L}. \tag{4}$$

Assuming that all the RISs are furnished with a uniform linear array (ULA) of M reflecting elements as well as a controller to intelligently adjust the phase shifts of reflecting elements with the aid of channel estimation and backhaul links.[4] Denoting $\mathbf{\Theta}_l = \text{diag}\{e^{j\theta_{l1}}, \cdots, e^{j\theta_{lm}}, \cdots, e^{j\theta_{lM}}\}$ as the diagonal phase-shift matrix for RIS l, where $\theta_{lm} \in [0, 2\pi), l \in \mathcal{L}, m \in \mathcal{M} = \{1, 2, \cdots, M\}$ is the phase shift of the i-th reflecting element of RIS l, and the phase shift θ_{lm} is assumed to be continuously controllable.

Assuming the links between the UAV to the RIS (U-R link) and the links between the RIS to the ground user (R-G link) are both LoS channels. Hence, the channel gain of the U-R link between UAV i and RIS l, denoted by $\boldsymbol{h}_{il}^{UR} \in \mathbb{C}^{M \times 1}$, is given by

$$\boldsymbol{h}_{il}^{UR} = h_{il}^{LoS}[1, e^{-j\frac{2\pi}{\lambda} d\vartheta_{il}}, \ldots, e^{-j\frac{2\pi}{\lambda}(M-1)d\vartheta_{il}}]^T, \tag{5}$$

where the vector is the array response of a M-element ULA, $\vartheta_{il} = \frac{a_l - x_i}{d_{il}}$ represents the cosine of the angle of arrival (AoA) of the signal from UAV i to the ULA at RIS l, the antenna

[3]In fact, we have to optimize UAVs' locations at each time slot in the actual scenario. In other words, the locations of UAVs change at every time slot. Therefore, UAVs in the considered model can be regarded as dynamic aerial base stations while they remain static in the duration of each time slot.

[4]The proposed algorithm can also be extended to the scenario in which each RIS is equipped with uniform rectangular array (URA) according to reference [39]. Without loss of generality, we investigate the scenario where each RIS is equipped with ULA in this paper.

separation and the carrier wavelength are represented by d and λ, respectively, d_{il} represents the distance between UAV i and RIS l. In (5), h_{il}^{LoS} represents the path loss of the U-R link which can be given based on the Lambertian emission model

$$h_{il}^{LoS} = \begin{cases} \frac{(k+1)A}{2\pi d_{il}^2} \cos^k(\phi_{il}) g(\varphi_{il}) \cos(\varphi_{il}), & 0 \le \varphi_{il} \le \Psi_c, \\ 0, & \varphi_{il} > \Psi_c, \end{cases} \tag{6}$$

where ϕ_{il} and φ_{il} represent the light emission and incidence angle from UAV i to RIS l, respectively.

Similarly, the channel gain of the R-G link between RIS l and ground user j, denoted by $\boldsymbol{h}_{lj}^{RG} \in \mathbb{C}^{M\times 1}$, is given by

$$\boldsymbol{h}_{lj}^{RG} = h_{lj}^{LoS}[1, e^{-j\frac{2\pi}{\lambda}d\vartheta_{lj}}, \ldots, e^{-j\frac{2\pi}{\lambda}(M-1)d\vartheta_{lj}}]^T, \tag{7}$$

where $\vartheta_{lj} = \frac{v_j - a_l}{d_{lj}}$ represents the cosine of the angle of departure (AoD) of the signal from RIS l to ground user j, d_{lj} represents the distance between RIS l and ground user j, h_{lj}^{LoS} represents the path loss of the R-G link which can also be expressed according to the Lambertian emission model

$$h_{lj}^{LoS} = \begin{cases} \frac{(k+1)A}{2\pi d_{lj}^2} \cos^k(\phi_{lj}) g(\varphi_{lj}) \cos(\varphi_{lj}), & 0 \le \varphi_{lj} \le \Psi_c, \\ 0, & \varphi_{lj} > \Psi_c, \end{cases} \tag{8}$$

where ϕ_{lj} and φ_{lj} represent the light emission and incidence angle from RIS l to ground user j, respectively.

After obtaining the channel gains of both the LoS links and the RIS-reflecting links, we further define the total channel gain as the sum of channel gain of LoS link and that of all the RIS-reflecting links. Mathematically, the total channel gain between UAV i and user j can be formulated by

$$h_j(\boldsymbol{q}_i) = \left| h_{ij}^{LoS} + \sum_{l=1}^{L} m_{il} (\boldsymbol{h}_{lj}^{RG})^H \boldsymbol{\Theta}_l \boldsymbol{h}_{il}^{UR} \right|, \tag{9}$$

where $\boldsymbol{q}_i = (x_i, y_i)$ represents the horizontal position of UAV i.

Considering that when terrestrial users are served by UAVs, they are all static, and the mobility and hovering energy consumption of all the UAVs is not taken into account in this paper. In our system model[5], multiple energy-constrained UAVs seek to find optimal deployment and resource allocation schemes that minimize their energy consumption on serving the requested downlink data requests.

B. Problem Formulation

Next, we first analyze the service requests and energy constraints in the system. Assuming the UAVs provide multi-cell channels to all the terrestrial users, the required data rate R_t for all the terrestrial users can be formulated by

$$\frac{1}{2}\log_2\left(1 + \frac{e}{2\pi}\left(\frac{\xi P_i h_j(\boldsymbol{q}_i)}{n_w}\right)^2\right) \ge R_t, \quad \forall i, j, \tag{10}$$

where e is Euler number, ξ is illumination response factor of transmitter, n_w denotes the power of additive noise. In (10), P_i represents the transmit power of UAV i. According to (10), we obtain the minimum transmit power of UAV i that meets the traffic rate demands of its serving users

$$P_i \ge \frac{u_{ij} n_w \sqrt{\frac{2\pi}{e}(2^{2R_t} - 1)}}{\xi h_j(\boldsymbol{q}_i)}, \quad \forall i, j. \tag{11}$$

With respect to the illumination requirements of terrestrial users served by UAV i, we have

$$\xi P_i h_j(\boldsymbol{q}_i) \ge u_{ij}\eta_j, \quad \forall j \in \mathcal{U}, \tag{12}$$

where η_j represents the illumination demand of ground user j.

Then, the joint deployment and resource allocation problem can be formulated as[6]

$$\min_{\boldsymbol{q}_i, \boldsymbol{u}_i, \boldsymbol{m}_i, \boldsymbol{\Theta}_t, P_i} \quad \sum_{i\in\mathcal{D}} P_i, \tag{13}$$

$$s.t. \quad \xi P_i h_j(\boldsymbol{q}_i) \ge u_{ij}\eta_j, \quad \forall i \in \mathcal{D}, \forall j \in \mathcal{U}, \tag{13a}$$

$$P_i \ge \frac{u_{ij} n_w \sqrt{\frac{2\pi}{e}(2^{2R_t} - 1)}}{\xi h_j(\boldsymbol{q}_i)}, \quad \forall i \in \mathcal{D}, \forall j \in \mathcal{U}, \tag{13b}$$

$$\sum_{i\in\mathcal{D}} u_{ij} = 1, \quad \forall j \in \mathcal{U}, \tag{13c}$$

$$\sum_{i\in\mathcal{D}} m_{il} = 1, \quad \forall l \in \mathcal{L}, \tag{13d}$$

$$u_{ij}, m_{il} \in \{0, 1\}, \quad \forall i \in \mathcal{D}, \forall j \in \mathcal{U}, \forall l \in \mathcal{L}, \tag{13e}$$

$$\|\boldsymbol{q}_i - \boldsymbol{q}_k\|^2 \ge d_{min}, \quad \forall i, k \in \mathcal{D}, i \ne k, \tag{13f}$$

where $\boldsymbol{u}_i = [u_{i1}, u_{i2}, \ldots, u_{iU}]$ denotes the user association vector of UAV i, $\boldsymbol{m}_i = [m_{i1}, m_{i2}, \ldots, m_{iL}]$ denotes the RIS association vector of UAV i, d_{min} is the predefined minimum distance between any two UAVs, and $\boldsymbol{\Theta}_t \in \mathbb{R}^{L\times M}$ denotes the phase shift matrix which is expressed as following:

$$\boldsymbol{\Theta}_t = \begin{bmatrix} \theta_{11} & \theta_{12} & \cdots & \theta_{1M} \\ \theta_{21} & \theta_{22} & \cdots & \theta_{2M} \\ \vdots & \vdots & \ddots & \vdots \\ \theta_{L1} & \theta_{L2} & \cdots & \theta_{LM} \end{bmatrix}. \tag{14}$$

In (13), the objective function denotes the sum transmit power of all UAVs. Constraint (13a) represents the illumination requirements of terrestrial users. The data requirement for each ground user is given in (13b). Constraint (13c) indicates that each ground user is served by at most one UAV. Each RIS can be located in only one UAV's aerial area as shown in (13d). Constraint (13e) represents the value space of integer variables. Constraint (13f) makes sure that the service areas do not overlap with each other.

As can be seen, problem (13) is non-convex due to the discrete user association and RIS association variables. Even

[5]Note that at every decision slot, the locations of UAVs shall be optimized to satisfy traffic and illumination requirements of users. The locations of UAVs not only affect the optimization of RISs phase shift, but also determine user and RIS association. Furthermore, due to the existence of RISs, there are two types of data transmission links: the direct LoS link and RIS-reflecting link. Hence, the considered system model is much more complicated than existing works [35], [36], [40]–[43], which shows that the conventional method cannot be directly applied to solve the problem associated to our system model.

[6]When it comes to day time, the terrestrial users will only have communication requirements without illumination requirements. Through setting the illumination requirements of users to zero, the new formulated optimization problem (13) is applicable to the dark time. Besides, the algorithm proposed in this paper is also efficient to solve this new problem. Therefore, our proposed model and algorithm are also applicable to day time.

for continuous variables, constraints (13a), (13b), and (13c) are still non-convex. Therefore, problem (13) is a NP-hard problem which is generally difficult to solve. Moreover, the coupling relationship between RISs phase shift and RIS association in total channel gain makes this problem more intractable.[7] To this end, an iterative algorithm is proposed to tackle with this problem. In particular, first, the optimizations of RISs phase shift in two application scenarios are solved by phase alignment method and SDP algorithm, respectively. Then, the non-convex UAV deployment problem is transformed through SCA method to a convex problem. And the problems of user and RIS association are solved using relaxation and dual techniques. Finally, we propose a greedy algorithm as an alternative to RIS association optimization with low complexity. Through alternately optimizing continuous and discrete variables, the solution of problem (13) can be obtained in polynomial complexity as can be seen in the next section.

III. Proposed Joint UAV Deployment, and User Association Solution

Next, we first introduce the proposed SDP and SCA-based algorithm which optimizes the deployment of UAVs and beamforming on RIS. Then, we explain how to use dual method and greedy method to optimize the association in the system.

A. Phase Shift Matrix Optimization and UAV Deployment

In this section, we optimize phase shift of RISs and UAV deployment with fixed user association and RIS association. Hence, the optimization problem (13) can be reduced to

$$\min_{\boldsymbol{q}_i,\boldsymbol{\Theta}_t,P_i} \sum_{i\in\mathcal{D}} P_i, \tag{15}$$

$$s.t.\quad P_i \geq \frac{A_j u_{ij}}{h_j(\boldsymbol{q}_i)},\quad \forall i\in\mathcal{D},\forall j\in\mathcal{U}, \tag{15a}$$

$$\|\boldsymbol{q}_i-\boldsymbol{q}_k\|^2 \geq d_{min},\quad \forall i,k\in\mathcal{D}, i\neq k, \tag{15b}$$

where $A_j=\max\left\{\frac{\eta_j}{\xi}, \frac{n_w\sqrt{\frac{2\pi}{e}(2^{2R_t}-1)}}{\xi}\right\}$. Due to the coupling relationship between phase shift of RISs and UAV deployment in the total channel gain, problem (15) can be settled in two steps: passive beamforming and UAV deployment optimization.

1) Passive Beamforming Optimization: Note that each UAV can serve one or more users based on user association and the algorithm for multi-user scenario [44] is far more complicated than that for single-user scenario [43]. To further reduce the computation complexity in passive beamforming optimization, we divide this subproblem in two application scenarios: only one user is associated with one UAV and more than one users are associated with one UAV.

[7]The prevalent machine learning method can be adopted to solve this problem, however, the large amount of labels to train neural network is not easy to obtain. Besides, the methods in existing works [35], [36], [40]–[43] can not be applied to solve this problem directly since the considered model is much more complicated and we have more variables to optimize.

a) Only one user is associated with UAV i: In this case, it is obviously that in order to maximize the received signal strength, the phases of the received signal shall be aligned at the ground user. Firstly, with fixed $\boldsymbol{q}_i$, the total channel gain $h_j(\boldsymbol{q}_i)$ in (9) can be further expressed by

$$h_j(\boldsymbol{q}_i)=\left|h_{ij}^{LoS}+\sum_{l\in\mathcal{L}_i} h_{lj}^{LoS}h_{il}^{LoS}\sum_{m=1}^{M} e^{j(\theta_{lm}+\frac{2\pi}{\lambda}d(m-1)(\vartheta_{lj}-\vartheta_{il}))}\right|, \tag{16}$$

where $\mathcal{L}_i=\{l\in\mathcal{L}|m_{il}=1\}$ denotes the set of RISs associated with UAV i. Therefore, signals from different paths are coherently combined at ground user j, i.e., $\theta_{l1}=\theta_{l2}+\frac{2\pi}{\lambda}d(\vartheta_{lj}-\vartheta_{il})=\cdots=\theta_{lM}+\frac{2\pi}{\lambda}d(M-1)(\vartheta_{lj}-\vartheta_{il})=0,\forall l\in\mathcal{L}_i$, or re-expressed by

$$\theta_{lm}=\frac{2\pi(m-1)d}{\lambda}(\vartheta_{il}-\vartheta_{lj}) \bmod 2\pi,\quad \forall l\in\mathcal{L}_i,\forall m\in\mathcal{M}. \tag{17}$$

That means the arriving signal's phase of every element from every associated RIS is the same for a ground user. In this way, the received signal energy is maximized through the phase alignment of received signals. Hence, $h_j(\boldsymbol{q}_i)$ can be further written as

$$h_j(\boldsymbol{q}_i)=h_{ij}^{LoS}+M\sum_{l\in\mathcal{L}_i} h_{lj}^{LoS}h_{il}^{LoS},\quad \forall i\in\mathcal{D},\forall j\in\mathcal{U}. \tag{18}$$

b) More than one users are associated with UAV i: When an UAV is serving more than one terrestrial users, the aligned phase $\boldsymbol{\Theta}_t$ will vary from one user to another if utilizing phase alignment method, thus brings the trouble to tackle with problem (15). With fixed $\boldsymbol{u}_i$, $\boldsymbol{m}_i$ and $\boldsymbol{q}_i$ in (15), the following problem is formulated for each UAV i $(i\in\mathcal{D})$:

$$\min_{\substack{\theta_{lm}\\ l\in\mathcal{L}_i,m\in\mathcal{M}}} \max_{j\in\mathcal{U}_i} \frac{A_j^2u_{ij}^2}{\left|h_{ij}^{LoS}+\sum_{l\in\mathcal{L}_i}(\boldsymbol{h}_{lj}^{RG})^H\boldsymbol{\Theta}_l\boldsymbol{h}_{il}^{UR}\right|^2}, \tag{19}$$
$$s.t.\quad \theta_{lm}\in[0,2\pi),\quad l\in\mathcal{L}_i,m\in\mathcal{M},$$

where $\mathcal{U}_i=\{j\in\mathcal{U}|u_{ij}=1\}$ denotes the set of terrestrial users associated with UAV i. Problem (19) is a nonlinear fractional programming which is equivalent to the following problem:

$$\min_{\substack{\theta_{lm}\\ l\in\mathcal{L}_i,m\in\mathcal{M}}} \max_{j\in\mathcal{U}_i} -\frac{\left|h_{ij}^{LoS}+\sum_{l\in\mathcal{L}_i}(\boldsymbol{h}_{lj}^{RG})^H\boldsymbol{\Theta}_l\boldsymbol{h}_{il}^{UR}\right|^2}{A_j^2u_{ij}^2}, \tag{20}$$
$$s.t.\quad \theta_{lm}\in[0,2\pi),\quad l\in\mathcal{L}_i,m\in\mathcal{M}.$$

To solve problem (20), we utilize semidefinite program (SDP) algorithm. Denote $z_{lm}=e^{-j\theta_{lm}}, \boldsymbol{z}_l=[z_{l1},\cdots,z_{lM}],\forall l,m$. Then $\boldsymbol{Z}_i\in\mathbb{C}^{|\mathcal{L}_i|\times M}$ represents the matrix of all the $\boldsymbol{z}_l$ that satisfy $l\in\mathcal{L}_i$ arranging in rows, where $|\mathcal{L}_i|$ represents the number of elements in set $\mathcal{L}_i$. The constraint in (20) is equal to $|z_{lm}|^2=1, l\in\mathcal{L}_i,m\in\mathcal{M}$. Through introducing $\boldsymbol{\Phi}_{ilj}=\text{diag}((\boldsymbol{h}_{lj}^{RG})^H)\boldsymbol{h}_{il}^{UR}\in\mathbb{C}^M$, $(\boldsymbol{h}_{lj}^{RG})^H\boldsymbol{\Theta}_l\boldsymbol{h}_{il}^{UR}$ can be transformed to $\boldsymbol{z}_l^*\boldsymbol{\Phi}_{ilj}$. Then, problem (20) can be further converted to

$$\min_{\boldsymbol{Z}_i}\max_{j\in\mathcal{U}_i} -\frac{1}{A_j^2u_{ij}^2}\left|h_{ij}^{LoS}+\sum_{l\in\mathcal{L}_i}\boldsymbol{z}_l^*\boldsymbol{\Phi}_{ilj}\right|^2, \tag{21}$$
$$s.t.\quad |\boldsymbol{z}_{lm}|^2=1,\quad l\in\mathcal{L}_i,m\in\mathcal{M}.$$

This article has been accepted for publication in a future issue of this journal, but has not been fully edited. Content may change prior to final publication. Citation information: DOI 10.1109/TWC.2022.3165853, IEEE Transactions on Wireless Communications

Since $h_{ij}^{LoS}+\sum_{l=1}^{L}\boldsymbol{z}_l^*\boldsymbol{\Phi}_{ilj}$ is a scalar, then we can obtain

$$\begin{aligned}&\left|h_{ij}^{LoS}+\sum_{l=1}^{L}\boldsymbol{z}_l^*\boldsymbol{\Phi}_{ilj}\right|^2\\ =&(h_{ij}^{LoS}+\sum_{l=1}^{L}\boldsymbol{z}_l^*\boldsymbol{\Phi}_{ilj})^H(h_{ij}^{LoS}+\sum_{l=1}^{L}\boldsymbol{z}_l^*\boldsymbol{\Phi}_{ilj}).\end{aligned}\tag{22}$$

Denote $\boldsymbol{\Phi}_{ij}^{(o)(p)}=\boldsymbol{\Phi}_{ioj}\boldsymbol{\Phi}_{ipj}^H$, $\hat{\boldsymbol{\Phi}}_{ioj}=h_{ij}^{LoS}\boldsymbol{\Phi}_{ioj}$, $\forall o,p\in\mathcal{L}_i$. Problem (21) can be further expressed as

$$\min_{\hat{\boldsymbol{z}}_i}\max_{j\in\mathcal{U}_i}\quad -\frac{1}{A_j^2u_{ij}^2}\left((h_{ij}^{LoS})^2+\hat{\boldsymbol{z}}_i^H\boldsymbol{Q}_{ij}\hat{\boldsymbol{z}}_i\right),\tag{23}$$

$$s.t.\quad |[\hat{\boldsymbol{z}}_i]_n|^2=1,\quad n=1,2,\cdots,|\mathcal{L}_i|M+1,\tag{23a}$$

where

$$\boldsymbol{Q}_{ij}=\begin{bmatrix}\boldsymbol{\Phi}_{ij}^{(1)(1)} & \boldsymbol{\Phi}_{ij}^{(1)(2)} & \cdots & \boldsymbol{\Phi}_{ij}^{(1)(|\mathcal{L}_i|)} & \hat{\boldsymbol{\Phi}}_{i1j}\\ \boldsymbol{\Phi}_{ij}^{(2)(1)} & \boldsymbol{\Phi}_{ij}^{(2)(2)} & \cdots & \boldsymbol{\Phi}_{ij}^{(2)(|\mathcal{L}_i|)} & \hat{\boldsymbol{\Phi}}_{i2j}\\ \vdots & \vdots & \ddots & \vdots & \vdots\\ \boldsymbol{\Phi}_{ij}^{(|\mathcal{L}_i|)(1)} & \boldsymbol{\Phi}_{ij}^{(|\mathcal{L}_i|)(2)} & \cdots & \boldsymbol{\Phi}_{ij}^{(|\mathcal{L}_i|)(|\mathcal{L}_i|)} & \hat{\boldsymbol{\Phi}}_{i|\mathcal{L}_i|j}\\ \hat{\boldsymbol{\Phi}}_{i1j}^H & \hat{\boldsymbol{\Phi}}_{i2j}^H & \cdots & \hat{\boldsymbol{\Phi}}_{i|\mathcal{L}_i|j}^H & 0\end{bmatrix},\tag{24}$$

$$\hat{\boldsymbol{z}}_i=\begin{bmatrix}\boldsymbol{z}_1^T\\ \vdots\\ \boldsymbol{z}_{|\mathcal{L}_i|}^T\\ 1\end{bmatrix}\in\mathbb{C}^{|\mathcal{L}_i|M+1}.\tag{25}$$

It can be inferred that $\hat{\boldsymbol{z}}_i^H\boldsymbol{Q}_{ij}\hat{\boldsymbol{z}}_i=tr(\hat{\boldsymbol{z}}_i^H\boldsymbol{Q}_{ij}\hat{\boldsymbol{z}}_i)=tr(\boldsymbol{Q}_{ij}\hat{\boldsymbol{z}}_i\hat{\boldsymbol{z}}_i^H)$, where $tr(\cdot)$ denotes matrix trace. In order to solve problem (23), we denote $\hat{\boldsymbol{z}}_i\hat{\boldsymbol{z}}_i^H$ as $\hat{\boldsymbol{Z}}_i\in\mathbb{C}^{(|\mathcal{L}_i|M+1)\times(|\mathcal{L}_i|M+1)}$ and $\hat{\boldsymbol{Z}}_i$ shall satisfy $\hat{\boldsymbol{Z}}_i\succeq\mathbf{0}$ and $rank(\hat{\boldsymbol{Z}}_i)=1$. Then, this rank-one constraint is relaxed to construct a SDP problem

$$\min_{\hat{\boldsymbol{Z}}_i}\max_{j\in\mathcal{U}_i}\quad -\frac{1}{A_j^2u_{ij}^2}\left((h_{ij}^{LoS})^2+tr(\boldsymbol{Q}_{ij}\hat{\boldsymbol{Z}}_i)\right),\tag{26}$$

$$s.t.\quad [\hat{\boldsymbol{Z}}_i]_{nn}=1,n=1,2,\cdots,|\mathcal{L}_i|M+1,\tag{26a}$$

$$\hat{\boldsymbol{Z}}_i\succeq 0.\tag{26b}$$

where (26) and (27) are linear, and the semi-definite constraint (26) is also convex according to [45]. Therefore, problem (26) is a standard convex problem, which can be effectively solved by using the CVX toolbox. Having the obtained solution of problem (26), we apply a rank-one approximation [45] on $\hat{\boldsymbol{Z}}_i$ to obtain $\hat{\boldsymbol{z}}_i$. Finally, $\boldsymbol{\Theta}_t$ can be obtained.

2) UAV deployment optimization: We further optimize the UAV deployment $\boldsymbol{q}_i$ with fixed $\boldsymbol{\Theta}_t$. Since $\|\boldsymbol{q}_i-\boldsymbol{q}_k\|^2$ in constraint (15b) is convex with respect to $\boldsymbol{q}_i$ and $\boldsymbol{q}_k$, we employ the first-order Taylor expansion to convert it into a linear function with respect to $\boldsymbol{q}_i$ and $\boldsymbol{q}_k$

$$\|\boldsymbol{q}_i-\boldsymbol{q}_k\|^2\geq 2(\boldsymbol{q}_i^{(r)}-\boldsymbol{q}_k^{(r)})^T(\boldsymbol{q}_i-\boldsymbol{q}_k)-\|\boldsymbol{q}_i^{(r)}-\boldsymbol{q}_k^{(r)}\|^2,\quad\forall i,k\in\mathcal{D},i\neq k,\tag{27}$$

where the superscript (r) represents the value at the previous iteration. Denote

$$g_0^r(\boldsymbol{q}_i-\boldsymbol{q}_k)\triangleq 2(\boldsymbol{q}_i^{(r)}-\boldsymbol{q}_k^{(r)})^T(\boldsymbol{q}_i-\boldsymbol{q}_k)-\|\boldsymbol{q}_i^{(r)}-\boldsymbol{q}_k^{(r)}\|^2,\tag{28}$$

which is a linear function with respect to $\boldsymbol{q}_i$ and $\boldsymbol{q}_k$. Then, substituting (28) into (15), problem (15) can be rewritten as

$$\min_{\boldsymbol{q}_i,P_i}\quad\sum_{i\in\mathcal{D}}P_i,\tag{29}$$

$$s.t.\quad P_i\geq\frac{A_ju_{ij}}{h_j(\boldsymbol{q}_i)},\quad\forall i\in\mathcal{D},\forall j\in\mathcal{U},\tag{29a}$$

$$g_0^r(\boldsymbol{q}_i-\boldsymbol{q}_k)\geq d_{min},\quad\forall i,k\in\mathcal{D},i\neq k,\tag{29b}$$

which is still non-convex due to the constraint (29a). To this end, we first introduce a group of new variables $\hat{h}_{ij},\forall i\in\mathcal{D},\forall j\in\mathcal{U}$. Then, problem (29) can be further expressed as

$$\min_{\boldsymbol{q}_i,P_i,\hat{h}_{ij}}\sum_{i\in\mathcal{D}}P_i,\tag{30}$$

$$s.t.\quad P_i\geq\frac{A_ju_{ij}}{\hat{h}_{ij}},\quad\forall i\in\mathcal{D},\forall j\in\mathcal{U},\tag{30a}$$

$$\hat{h}_{ij}\leq h_j(\boldsymbol{q}_i),\quad\forall i\in\mathcal{D},\forall j\in\mathcal{U},\tag{30b}$$

$$g_0^r(\boldsymbol{q}_i-\boldsymbol{q}_k)\geq d_{min},\quad\forall i,k\in\mathcal{D},i\neq k,\tag{30c}$$

where (30a) is convex, but (30b) is non-convex. Substituting (9) into (30b), we can obtain

$$\hat{h}_{ij}\leq\left|h_{ij}^{LoS}+\sum_{l=1}^{L}m_{il}(\boldsymbol{h}_{lj}^{RG})^H\boldsymbol{\Theta}_l\boldsymbol{h}_{il}^{UR}\right|=\left|h_{ij}^{LoS}+\sum_{l=1}^{L}\kappa_{ilj}^{(r)}h_{il}^{LoS}\right|,\tag{31}$$

where $\kappa_{ilj}^{(r)}$ is the coefficient of h_{il}^{LoS} that can be approximated by using the AoA of the signal at RIS at the previous iteration. In (31), only h_{ij}^{LoS} and h_{il}^{LoS} are related with $\boldsymbol{q}_i$. Thus, we can further introduce a new group of variables $\hat{h}_{ij}^{LoS},\hat{h}_{il}^{LoS},\forall i,l,j$ into problem (30)

$$\min_{\boldsymbol{q}_i,P_i,\hat{h}_{ij},\hat{h}_{ij}^{LoS},\hat{h}_{il}^{LoS}}\quad\sum_{i\in\mathcal{D}}P_i,\tag{32}$$

$$s.t.\quad P_i\geq\frac{A_ju_{ij}}{\hat{h}_{ij}},\quad\forall i\in\mathcal{D},\forall j\in\mathcal{U},\tag{32a}$$

$$\hat{h}_{ij}\leq\left|\hat{h}_{ij}^{LoS}+\sum_{l=1}^{L}\kappa_{ilj}^{(r)}\hat{h}_{il}^{LoS}\right|,\quad\forall i\in\mathcal{D},\forall j\in\mathcal{U},\tag{32b}$$

$$g_0^r(\boldsymbol{q}_i-\boldsymbol{q}_k)\geq d_{min},\quad\forall i,k\in\mathcal{D},i\neq k,\tag{32c}$$

$$\hat{h}_{ij}^{LoS}\leq\frac{(k+1)A}{2\pi d_{ij}^2}\cos^k(\phi_{ij}^{(r)})g(\varphi_{ij}^{(r)})\cos(\varphi_{ij}^{(r)}),\quad\forall i\in\mathcal{D},\forall j\in\mathcal{U},\tag{32d}$$

$$\hat{h}_{il}^{LoS}\leq\frac{(k+1)A}{2\pi d_{il}^2}\cos^k(\phi_{il}^{(r)})g(\varphi_{il}^{(r)})\cos(\varphi_{il}^{(r)}),\quad\forall i\in\mathcal{D},\forall l\in\mathcal{L},\tag{32e}$$

where $\phi_{ij}^{(r)}$ and $\varphi_{ij}^{(r)}$ represent the emission and incidence angle at the previous iteration, respectively. Due to constraints (32b), (32d) and (32e) are still non-convex, we also use the

first-order Taylor expansion method as that in (27). Then problem (32) can be transformed into the following problem:

$$\min_{\boldsymbol{q}_i,P_i,\hat{h}_{ij},\hat{h}_{ij}^{LoS},\hat{h}_{il}^{LoS}} \quad \sum_{i\in\mathcal{D}} P_i, \tag{33}$$

$$s.t. \quad P_i \geq \frac{A_j u_{ij}}{\hat{h}_{ij}}, \quad \forall i \in \mathcal{D}, \forall j \in \mathcal{U}, \tag{33a}$$

$$g_0^r(\boldsymbol{q}_i - \boldsymbol{q}_k) \geq d_{min}, \quad \forall i,k \in \mathcal{D}, i \neq k, \tag{33b}$$

$$g_1^r(\hat{h}_{ij}^{LoS}, \hat{h}_{il}^{LoS}) \geq \hat{h}_{ij}^2, \quad \forall i \in \mathcal{D}, \forall j \in \mathcal{U}, \tag{33c}$$

$$g_2^r(\hat{h}_{ij}^{LoS}) \geq d_{ij}^2, \quad \forall i \in \mathcal{D}, \forall j \in \mathcal{U}, \tag{33d}$$

$$g_3^r(\hat{h}_{il}^{LoS}) \geq d_{il}^2, \quad \forall i \in \mathcal{D}, \forall l \in \mathcal{L}, \tag{33e}$$

where

$$g_1^r(\hat{h}_{ij}^{LoS}, \hat{h}_{il}^{LoS}) = 2\mathrm{Re}\left\{\left((\hat{h}_{ij}^{LoS})^{(r)} + \sum_{l=1}^{L} \kappa_{ilj}^{(r)} (\hat{h}_{il}^{LoS})^{(r)}\right)^* \left(\hat{h}_{ij}^{LoS} + \sum_{l=1}^{L} \kappa_{ilj}^{(r)} \hat{h}_{il}^{LoS}\right)\right\} - \left|(\hat{h}_{ij}^{LoS})^{(r)} + \sum_{l=1}^{L} \kappa_{ilj}^{(r)} (\hat{h}_{il}^{LoS})^{(r)}\right|^2 \quad \forall i \in \mathcal{D}, \forall j \in \mathcal{U}, \tag{34}$$

$$g_2^r(\hat{h}_{ij}^{LoS}) = \frac{(k+1)A\left[2 \times (\hat{h}_{ij}^{LoS})^{(r)} - \hat{h}_{ij}^{LoS}\right]}{2\pi\left((\hat{h}_{ij}^{LoS})^{(r)}\right)^2} \times \cos^k(\phi_{ij}^{(r)}) g(\varphi_{ij}^{(r)}) \cos(\varphi_{ij}^{(r)}), \quad \forall i \in \mathcal{D}, \forall j \in \mathcal{U}, \tag{35}$$

$$g_3^r(\hat{h}_{il}^{LoS}) = \frac{(k+1)A\left[2 \times (\hat{h}_{il}^{LoS})^{(r)} - \hat{h}_{il}^{LoS}\right]}{2\pi\left((\hat{h}_{il}^{LoS})^{(r)}\right)^2} \times \cos^k(\phi_{il}^{(r)}) g(\varphi_{il}^{(r)}) \cos(\varphi_{il}^{(r)}), \quad \forall i \in \mathcal{D}, \forall l \in \mathcal{D}, \tag{36}$$

which are all linear functions with all the $(\cdot)^{(r)}$ stands for the value of $(\cdot)$ at the previous iteration. Problem (33) is now convex which can be figured out the global optimal solution by using CVX toolbox.

In summery, by the proposed SDP and SCA-based algorithm, the deployment of UAVs and beamforming on RIS are respectively optimized. However, to reach the optimal communication performance, the optimization of user and RIS association must be studied.

B. User Association and RIS Association Optimization

In this subsection, we introduce an optimal closed-form solution that optimize the association in the system. In particular, we will optimize user association and RIS association with fixed UAVs deployment and RISs beamforming. Thus, the optimization problem (13) can be reduced to

$$\min_{\boldsymbol{u}_i,\boldsymbol{m}_i,P_i} \sum_{i\in\mathcal{D}} P_i, \tag{37}$$

$$s.t. \quad P_i \geq \frac{A_j u_{ij}}{h_j(\boldsymbol{q}_i)}, \quad \forall i \in \mathcal{D}, \forall j \in \mathcal{U}, \tag{37a}$$

$$\sum_{i\in\mathcal{D}} u_{ij} = 1, \quad \forall j \in \mathcal{U}, \tag{37b}$$

$$\sum_{i\in\mathcal{D}} m_{il} = 1, \quad \forall l \in \mathcal{L}, \tag{37c}$$

$$u_{ij}, m_{il} \in \{0,1\}, \quad \forall i \in \mathcal{D}, \forall j \in \mathcal{U}, \forall l \in \mathcal{L}. \tag{37d}$$

Because of the coupling relationship between user association and RIS association in (37a), problem (37) can be solved in two steps: user association optimization and RIS association optimization.

1) User Association Optimization: With fixed RIS Association $\boldsymbol{m}_i$, we adopt the fractional relaxation method to make this combinatorial problem tractable. In this case, $\boldsymbol{u}_i$ can take on any real value in $[0,1]$. Thus, problem (37) can be reformulated as

$$\min_{\boldsymbol{u}_i,P_i} \sum_{i\in\mathcal{D}} P_i, \tag{38}$$

$$s.t. \quad P_i \geq \frac{A_j u_{ij}}{h_j(\boldsymbol{q}_i)}, \quad \forall i \in \mathcal{D}, \forall j \in \mathcal{U}, \tag{38a}$$

$$\sum_{i\in\mathcal{D}} u_{ij} = 1, \quad \forall j \in \mathcal{U}, \tag{38b}$$

$$u_{ij} \geq 0, \quad \forall i \in \mathcal{D}, \forall j \in \mathcal{U}, \tag{38c}$$

which is a linear programming problem. And the dual problem of (38) is given by

$$\max_{\boldsymbol{\beta}} \quad D(\boldsymbol{\beta}), \tag{39}$$

where

$$D(\boldsymbol{\beta}) = \begin{cases} \min\limits_{\boldsymbol{u}_i,P_i} \quad L(\boldsymbol{u}_i, P_i, \boldsymbol{\beta}), \\ s.t. \quad \sum\limits_{i\in\mathcal{D}} u_{ij} = 1, \quad \forall j \in \mathcal{U}, \\ \qquad u_{ij} \geq 0, \quad \forall i \in \mathcal{D}, \forall j \in \mathcal{U}, \end{cases} \tag{40}$$

with

$$L(\boldsymbol{u}_i, P_i, \boldsymbol{\beta}) = \sum_{i\in\mathcal{D}} P_i + \sum_{i\in\mathcal{D}} \sum_{j\in\mathcal{U}} \beta_{ij} \left(\frac{A_j u_{ij}}{h_j(\boldsymbol{q}_i)} - P_i\right), \tag{41}$$

and $\boldsymbol{\beta} = \{\beta_{ij} | \forall i \in \mathcal{D}, \forall j \in \mathcal{U}\}$ is non-negative relaxation variables with respect to (38a). In order to minimize this linear objective function of (39), we set the smallest association coefficient corresponding to the u_{ij} be 1 among all the UAVs with the given ground user j. Hence, we can obtain the optimal u_{ij}^*

$$u_{ij}^* = \begin{cases} 1, & \text{if} \quad i = \arg\min\limits_{i\in\mathcal{D}} \dfrac{\beta_{ij} A_j}{h_j(\boldsymbol{q}_i)}, \\ 0, & \text{otherwise.} \end{cases} \tag{42}$$

If there are multiple indexes in satisfying $\arg\min_{i\in\mathcal{D}} \frac{\beta_{ij} A_j}{h_j(\boldsymbol{q}_i)}$, we can choose any one of them.

This article has been accepted for publication in a future issue of this journal, but has not been fully edited. Content may change prior to final publication. Citation information: DOI 10.1109/TWC.2022.3165853, IEEE Transactions on Wireless Communications

To achieve the optimal P_i^* from (40), we take the first derivative with respect to P_i considering that (40) is a linear problem with respect to P_i

$$\frac{\partial L(\boldsymbol{u}_i, P_i, \boldsymbol{\beta})}{\partial P_i} = 1 - \sum_{j\in\mathcal{U}} \beta_{ij}. \tag{43}$$

Notice that the optimal $P_i^* = +\infty$ if $1 - \sum_{j\in\mathcal{U}} \beta_{ij} < 0$. To avoid that, we let $\sum_{j\in\mathcal{U}} \beta_{ij} \leq 1$. Then the optimal P_i^* can be obtained

$$P_i^* = \max_{j\in\mathcal{U}} \frac{A_j u_{ij}}{h_j(\boldsymbol{q}_i)}, \quad \forall i \in \mathcal{D}. \tag{44}$$

The value of β_{ij} can be updated by the gradient method

$$\beta_{ij} = \left[\beta_{ij}^{(r)} + \rho\left(\frac{A_j u_{ij}^{(r)}}{h_j(\boldsymbol{q}_i)} - P_i^{(r)}\right)\right]^+, \quad \forall i \in \mathcal{D}, \forall j \in \mathcal{U}, \tag{45}$$

where all the $(\cdot)^{(r)}$ stands for the value of $(\cdot)$ at the previous iteration, $[a]^+ = \max(a, 0)$, and ρ is a dynamically positive step-size factor. Since problem (38) is convex and Slater's condition is satisfied, strong duality between primal problem (38) and dual problem (39) holds. Thus, the optimal $\boldsymbol{u}_i^*$ and P_i^* with fixed $\boldsymbol{m}_i$ can be obtained through iteratively optimizing primal variables and dual variables.

From (42), we can find that although the feasible range of u_{ij} is relaxed to be continuous, the optimal solution to problem (38) always satisfies the discrete constraint $u_{ij} \in \{0, 1\}, \forall i \in \mathcal{D}, \forall j \in \mathcal{U}$. Hence, the relaxation of u_{ij} does not lose optimality to the primal problem (38).

2) RIS Association Optimization: We now optimize RIS association with fixed user association. In particular, we propose two efficient algorithms, dual method and greedy algorithm, to tackle RIS association problem.

a) Dual Method: First, we formulate the following optimization problem respect to $\boldsymbol{m}_i$:

$$\min_{\boldsymbol{m}_i, \tilde{h}_{ij}, P_i} \sum_{i\in\mathcal{D}} P_i, \tag{46}$$

$$s.t. \quad P_i \geq \frac{A_j u_{ij}}{\tilde{h}_{ij}}, \quad \forall i \in \mathcal{D}, \forall j \in \mathcal{U}, \tag{46a}$$

$$\tilde{h}_{ij} \leq \left| h_{ij}^{LoS} + \sum_{l=1}^{L} m_{il} (\boldsymbol{h}_{lj}^{RG})^H \boldsymbol{\Theta}_l \boldsymbol{h}_{il}^{UR} \right|, \quad \forall i \in \mathcal{D}, \forall j \in \mathcal{U}, \tag{46b}$$

$$\sum_{i\in\mathcal{D}} m_{il} = 1, \quad \forall l \in \mathcal{L}, \tag{46c}$$

$$m_{il} \in \{0, 1\}, \quad \forall i \in \mathcal{D}, \forall l \in \mathcal{L}, \tag{46d}$$

where $\{\tilde{h}_{ij} | \forall i, j\}$ is a group of new introduced variables. Note that for the optimality of problem (46), constraint (46b) will always hold with equality. Due to the non-convexity of constraint (46b), we first rewrite the right hand side of constraint (46b) due to the fact that $m_{il} \in \{0, 1\}$

$$\left| h_{ij}^{LoS} + \sum_{l=1}^{L} m_{il} (\boldsymbol{h}_{lj}^{RG})^H \boldsymbol{\Theta}_l \boldsymbol{h}_{il}^{UR} \right|^2 = C_{ij0} + \sum_{l=1}^{L} C_{ijl} m_{il} + \sum_{l=2}^{L} \sum_{v=1}^{l-1} C_{ijlv} m_{il} m_{iv}, \tag{47}$$

where $C_{ij0}, C_{ijl}, C_{ijlv}$ are the corresponding coefficients, i.e.,

$$\begin{aligned} C_{ij0} &= (h_{ij}^{LoS})^2, \\ C_{ijl} &= 2h_{ij}^{LoS} \mathrm{Re}\{(\boldsymbol{h}_{lj}^{RG})^H \boldsymbol{\Theta}_l \boldsymbol{h}_{il}^{UR}\} + \left|(\boldsymbol{h}_{lj}^{RG})^H \boldsymbol{\Theta}_l \boldsymbol{h}_{il}^{UR}\right|^2, \\ C_{ijlv} &= 2\mathrm{Re}\{(\boldsymbol{h}_{il}^{UR})^H \boldsymbol{\Theta}_l^H \boldsymbol{h}_{lj}^{RG} (\boldsymbol{h}_{vj}^{RG})^H \boldsymbol{\Theta}_v \boldsymbol{h}_{iv}^{UR}\}. \end{aligned} \tag{48}$$

Due to the existence of quadratic terms in (47), we denote $m_{il} m_{iv}$ as E_{ilv} $(\forall i \in \mathcal{D}, \forall l, v \in \mathcal{L}, l < v)$. Thus, E_{ilv} must satisfies

$$\begin{aligned} &E_{ilv} \geq m_{il} + m_{iv} - 1, 0 \leq E_{ilv} \leq 1, \\ &E_{ilv} \leq m_{il}, m_{iv}, \quad \forall i \in \mathcal{D}, \forall l, v \in \mathcal{L}, l < v. \end{aligned} \tag{49}$$

Now, problem (46) can be reformulated as

$$\min_{\boldsymbol{m}_i, \tilde{h}_{ij}, E_{ilv}, P_i} \sum_{i\in\mathcal{D}} P_i, \tag{50}$$

$$s.t. \quad P_i \geq \frac{A_j u_{ij}}{\tilde{h}_{ij}}, \quad \forall i \in \mathcal{D}, \forall j \in \mathcal{U}, \tag{50a}$$

$$\tilde{h}_{ij}^2 \leq C_{ij0} + \sum_{l=1}^{L} C_{ijl} m_{il} + \sum_{l=2}^{L} \sum_{v=1}^{l-1} C_{ijlv} E_{ilv}, \quad \forall i \in \mathcal{D}, \forall j \in \mathcal{U}, \tag{50b}$$

$$E_{ilv} \geq m_{il} + m_{iv} - 1, 0 \leq E_{ilv} \leq 1, \quad \forall i \in \mathcal{D}, \forall l, v \in \mathcal{L}, l < v, \tag{50c}$$

$$E_{ilv} \leq m_{il}, m_{iv}, \quad \forall i \in \mathcal{D}, \forall l, v \in \mathcal{L}, l < v, \tag{50d}$$

$$\sum_{i\in\mathcal{D}} m_{il} = 1, \quad \forall l \in \mathcal{L}, \tag{50e}$$

$$m_{il} \geq 0, \quad \forall i \in \mathcal{D}, \forall l \in \mathcal{L}, \tag{50f}$$

where we have relaxed the integer constraints (46d) with $m_{il} \in [0, 1]$. Thus, problem (50) becomes convex which can be tracked by the dual method.

The dual problem of (50) is given by

$$\max_{\boldsymbol{\tau}, \boldsymbol{\gamma}, \boldsymbol{\Gamma}} \hat{D}(\boldsymbol{\tau}, \boldsymbol{\gamma}, \boldsymbol{\Gamma}), \tag{51}$$

where

$$\hat{D}(\boldsymbol{\tau}, \boldsymbol{\gamma}, \boldsymbol{\Gamma}) = \begin{cases} \min\limits_{\boldsymbol{m}_i, \tilde{h}_{ij}, E_{ilv}, P_i} \hat{L}(\boldsymbol{m}_i, \tilde{h}_{ij}, E_{ilv}, P_i, \boldsymbol{\tau}, \boldsymbol{\gamma}, \boldsymbol{\Gamma}), \\ s.t. \quad \sum\limits_{i\in\mathcal{D}} m_{il} = 1, \quad \forall l \in \mathcal{L}, \\ \qquad m_{il} \geq 0, \quad \forall i \in \mathcal{D}, \forall l \in \mathcal{L}, \\ \qquad 0 \leq E_{ilv} \leq 1, \forall i \in \mathcal{D}, \forall l, v \in \mathcal{L}, l < v, \end{cases} \tag{52}$$

with

$$\begin{aligned} \hat{L}(\boldsymbol{m}_i, \tilde{h}_{ij}, E_{ilv}, P_i, \boldsymbol{\tau}, \boldsymbol{\gamma}, \boldsymbol{\Gamma}) &= \sum_{i\in\mathcal{D}} P_i - \sum_{i\in\mathcal{D}} \sum_{j\in\mathcal{U}} \left[\tau_{ij}\left(P_i - \frac{A_j u_{ij}}{\tilde{h}_{ij}}\right)\right] \\ &- \sum_{i\in\mathcal{D}} \sum_{j\in\mathcal{U}} \left[\gamma_{ij}\left(C_{ij0} + \sum_{l=1}^{L} C_{ijl} m_{il} + \sum_{l=2}^{L} \sum_{v=1}^{l-1} C_{ijlv} E_{ilv} - \tilde{h}_{ij}^2\right)\right] \\ &- \sum_{i\in\mathcal{D}} \sum_{l=2}^{L} \sum_{v=1}^{l-1} \left[\Gamma_{1ilv}(E_{ilv} - m_{il} - m_{iv} + 1) + \Gamma_{2ilv}(m_{il} - E_{ilv}) \right. \\ &\left. + \Gamma_{3ilv}(m_{iv} - E_{ilv})\right], \end{aligned} \tag{53}$$

This article has been accepted for publication in a future issue of this journal, but has not been fully edited. Content may change prior to final publication. Citation information: DOI 10.1109/TWC.2022.3165853, IEEE Transactions on Wireless Communications

and $\boldsymbol{\tau} = \{\tau_{ij}\}$, $\boldsymbol{\gamma} = \{\gamma_{ij}\}$ and $\boldsymbol{\Gamma} = \{\Gamma_{1ilv}, \Gamma_{2ilv}, \Gamma_{3ilv}\}$ are non-negative Lagrange multipliers with respect to the corresponding constraints in primal problem (50).

Similarly, to minimize the linear objective function in (52), we set the positive coefficients corresponding to the E_{ilv} be 0

$$E^*_{ilv} = \begin{cases} 1, & \text{if } \Gamma_{1ilv} - \Gamma_{2ilv} - \Gamma_{3ilv} + \sum_{j\in\mathcal{U}} \gamma_{ij} C_{ijlv} > 0, \\ 0, & \text{otherwise.} \end{cases} \tag{54}$$

Due to the constraint $\sum_{i\in\mathcal{D}} m_{il} = 1, \forall l \in \mathcal{L}$, we set the smallest association coefficient corresponding to m_{il} be 1 among all the UAVs with given RIS l

$$m^*_{il} = \begin{cases} 1, & \text{if } i = \arg\min_{i\in\mathcal{D}} C_{il}, \\ 0, & \text{otherwise,} \end{cases} \tag{55}$$

where

$$C_{il} = \begin{cases} -\sum_{j\in\mathcal{U}} \gamma_{ij} C_{ijl} - \sum_{v=2}^{L} (\Gamma_{3ilv} - \Gamma_{1ilv}), & \text{if } l = 1, \\ -\sum_{j\in\mathcal{U}} \gamma_{ij} C_{ijl} - \sum_{v=1}^{l-1} (\Gamma_{2ilv} - \Gamma_{1ilv}) - \sum_{v=l+1}^{L} (\Gamma_{3ilv} - \Gamma_{1ilv}), & \\ \qquad\qquad \text{if } 2 \le l \le L-1, & \\ -\sum_{j\in\mathcal{U}} \gamma_{ij} C_{ijl} - \sum_{v=1}^{L-1} (\Gamma_{2ilv} - \Gamma_{1ilv}), & \text{if } l = L. \end{cases} \tag{56}$$

The optimal RIS association (55) indicates that the RIS will chose the optimal UAV to associate based on large value of channel coefficient C_{ijl}.

The optimal $\tilde{h}_{ij}$ can be achieved through setting the first derivative of (53) with respect to $\tilde{h}_{ij}$ to 0

$$\tilde{h}_{ij} = \sqrt[3]{\frac{\tau_{ij} A_j u_{ij}}{2\gamma_{ij}}}, \quad \forall i \in \mathcal{D}, \forall j \in \mathcal{U}. \tag{57}$$

Therefore, the optimal $P^*_i, \forall i \in \mathcal{D}$ takes the minimum value that satisfies (50a).

The values of $\boldsymbol{\tau} = \{\tau_{ij}\}$, $\boldsymbol{\gamma} = \{\gamma_{ij}\}$ and $\boldsymbol{\Gamma} = \{\Gamma_{1ilv}, \Gamma_{2ilv}, \Gamma_{3ilv}\}$ can be given by the sub-gradient method

$$\tau_{ij} = \left[\tau_{ij} - \rho\left(P_i - \frac{A_j u_{ij}}{\tilde{h}_{ij}}\right)\right]^+, \tag{58}$$

$$\gamma_{ij} = \left[\gamma_{ij} - \rho\left(C_{ij0} + \sum_{l=1}^{L} C_{ijl} m_{il} + \sum_{l=2}^{L}\sum_{v=1}^{l-1} C_{ijlv} E_{ilv} - \tilde{h}^2_{ij}\right)\right]^+$$

$$\Gamma_{1ilv} = [\Gamma_{1ilv} - \rho(E_{ilv} - m_{il} - m_{iv} + 1)]^+,$$

$$\Gamma_{2ilv} = [\Gamma_{2ilv} - \rho(m_{il} - E_{ilv})]^+,$$

$$\Gamma_{3ilv} = [\Gamma_{3ilv} - \rho(m_{iv} - E_{ilv})]^+.$$

Since problem (50) is convex and Slater's condition is satisfied, strong duality between primal problem (50) and dual problem (51) holds. Therefore, we can obtain the optimal $\boldsymbol{m}^*_{il}$ and P^*_i with fixed $\boldsymbol{u}_{ij}$ through optimizing primal variables and dual variables iteratively. From (55), we can find that although the feasible range of u_{ij} is relaxed to be continuous, the optimal solution to problem (46) always satisfies the discrete constraint $u_{ij} \in \{0, 1\}, \forall i \in \mathcal{D}, \forall j \in \mathcal{U}$. Hence, relaxation of u_{ij} does not lose optimality to the primal problem (46).

Algorithm 1 Greedy Algorithm for RIS Association Optimization

1: **Input:** user association $\boldsymbol{u}_i$, phase shift matrix $\boldsymbol{\Theta}_t$,UAV deployment $\boldsymbol{q}_i$.
2: **Initialize:** $m_{il} = 0, \forall i \in \mathcal{D}, \forall l \in \mathcal{L}$.
3: **For** $l = 1 : 1 : L$ **do**
4: $\quad i^* = \arg\min_{i\in\mathcal{D}} \sum_{i\in\mathcal{D}} P_i$,
5: $\quad m_{i^*l} = 1$,
6: **End**
7: **Output:** RIS association $\boldsymbol{m}_i$.

Algorithm 2 Iterative Beamforming, Deployment, and Association Algorithm

1: **Input:** terrestrial users' locations, altitude of UAV H, data rate requirement R_t, illumination requirement η_j.
2: **Initialize:** $\boldsymbol{u}_i$, $\boldsymbol{m}_i$, $\boldsymbol{q}_i$.
3: **repeat**
4: Passive Beamforming Optimization $\boldsymbol{\Theta}_t$:
if Only one user is associated with UAV i:
then solve (17);
else:
then solve (26) using (25).
5: UAV deployment optimization $\boldsymbol{q}_i$:
Solve (33) using (28), (34)-(36).
6: User Association Optimization $\boldsymbol{u}_i$:
Solve (42)
Update $\boldsymbol{\beta}$ using (45).
7: RIS Association Optimization $\boldsymbol{m}_i$:
if using dual method:
then solve (17);
Solve (55) using (48), (56)
Update $\boldsymbol{\tau}$, $\boldsymbol{\gamma}$, $\boldsymbol{\Gamma}$ using (54), (57), (58).
if using greedy algorithm:
then conduct Algorithm 1.
8: **until** the objective value (13) converges.
9: **Output:** $\boldsymbol{u}_i$, $\boldsymbol{m}_i$, $\boldsymbol{q}_i$, $\boldsymbol{\Theta}_t$.

b) Greedy Algorithm: To optimize the RIS association with low complexity, we propose a greedy algorithm that optimizes the association at each RIS successively. In particular, there is no RIS associated with any UAV at the beginning. Then, step by step, one RIS is added and associated with one UAV, for the best energy usage efficiency. This algorithm does not terminate until all the L RISs are associated. The details of our greedy algorithm are listed as Algorithm 1. Since the greedy algorithm obtains the optimal association at each RIS successively which cannot guarantee the global optimality of all the RIS association, the outcome of this algorithm is a local optimal solution.

C. Complexity and Analysis

We summarize the proposed algorithm to solve problem (13) in Algorithm 2. The complexity of Algorithm 2 consists of solving four subproblems: RISs phase shift subproblem, UAV deployment subproblem, user association subproblem and RIS association subproblem. For the RISs phase shift optimization, we consider two situations: if only one user is associated with UAV i, the complexity of calculating θ_{lm} is $\mathcal{O}(LM)$ according to (17), otherwise, the complexity of

solving an SDP optimization problem (26) is $\mathcal{O}\left((LM+1)^3\right)$. For the UAV deployment optimization, we use SCA method to tackle this sub-problem, the complexity at each iteration is $\mathcal{O}(S_1^2 S_2)$, where $S_1 = 2DU + DL + 3D$ denotes the total number of variables and $S_2 = \frac{D(D-1)}{2} + 3DU + DL$ represents the total number of constraints. To solve the UAV deployment problem, the number of iterations required for SCA is $\mathcal{O}\left(\sqrt{S_1}\log_2(1/\epsilon_1)\right)$, where ϵ_1 is the accuracy of SCA. And the complexity of UAV deployment can be given by $\mathcal{O}(S_1^{2.5} S_2 \log_2(1/\epsilon_1))$. For the user association optimization, the complexity of calculating (42) is $\mathcal{O}(DU)$. The iteration number of the user association problem is estimated by $\mathcal{O}(1/\sqrt{\epsilon_2})$, where ϵ_2 denotes the precision of the dual method in this sub-problem. And the complexity of user association is given by $\mathcal{O}(DU/\sqrt{\epsilon_2})$. For the RIS association optimization, in the case of using the dual method, the complexity of calculating (55) is $\mathcal{O}(DL)$. Besides, the iteration number until (50) converges can be estimated as $\mathcal{O}(1/\sqrt{\epsilon_3})$, where ϵ_3 represents the precision of dual method adopted in this sub-problem. In the case of using greedy algorithm, the complexity is $\mathcal{O}(DL)$. The total complexities of the proposed Algorithm 2 with dual method and greedy algorithm in RIS association optimization are $\mathcal{O}\left(\hat{L}[(LM+1)^3 + S_1^{2.5} S_2 \log_2(1/\epsilon_1) + \frac{DU}{\sqrt{\epsilon_2}} + \frac{DL}{\sqrt{\epsilon_3}}]\right)$ and $\mathcal{O}\left(\hat{L}[(LM+1)^3 + S_1^{2.5} S_2 \log_2(1/\epsilon_1) + DU/\sqrt{\epsilon_2} + DL]\right)$, respectively, where $\hat{L}$ is the iteration number of the proposed iterative algorithm. In conclusion, the calculation of the proposed optimization algorithms only requires polynomial computational complexity. For the RIS association optimization problem, the computation complexity of greedy algorithm is smaller compared to the dual method.

Since we alternately optimize beamforming on RISs, deployment of UAVs, user association and RIS association, the solution is not global optimal but a sub-optimal solution instead. And the optimality is difficult to deduce in theory. However, the optimization of beamforming on RISs in case of only one user is associated with one UAV, user association and RIS association can be proved to achieve the optimal solutions, respectively. And the SDP method to solve RISs phase shifts in case of multiple users are associated with one UAV can guarantee at least a $\frac{\pi}{4}$-approximation of the optimal solution according to reference [22]. In the next section, we will show that the gaps between the proposed schemes and the global optimal scheme are small, which indicates that the proposed schemes approach the optimal solution.

From this section we can see that the proposed algorithms are both totally centralized since the control center of this network needs to know the channel states of all the UAV-user and UAV-RIS-user links, users and RISs locations as well as users demand for traffic and illumination. All these needed information shall be first fed back to the control center through the backhaul links. Then after the implementation of the proposed algorithms, the optimal RISs beamforming, UAV deployment, user association and RIS association are sent to the corresponding nodes through fronthual links to serve terrestrial users.

TABLE I: Simulation Parameters

Parameters	Symbols	Values
Semi-angle	$\Phi_{\frac{1}{2}}$	80°
Detecting area of each receiver	A	1cm^2
Altitude of UAVs	H	20m
Field of view	Ψ_c	90°
Internal reflective index	n	4.5
Altitude of RISs	z_R	5m
Minimum distance between two UAVs	d_{min}	10m
Illumination response factor of transmitter	ξ	0.9Amp./W
Power of AWGN	n_w	1×10^{-12}

IV. Simulation Results

In this section, simulations are performed to corroborate the performance of our proposed algorithms. A 100m $\times$ 100m square area is considered with $U = 9$ randomly deployed terrestrial users. $L = 3$ RISs which has $M = 12$ reflecting elements and $D = 3$ UAVs are also deployed in this specific area. The required data rate for all the terrestrial users is $R_t = 25$bps/Hz and the illumination requirements of all the terrestrial users are generated randomly and uniformly over $[10^{-5}, 9 \times 10^{-5}]$. Moreover, the antenna separation d equals to a half of the carrier wavelength λ. Table I lists other parameters. Additionally, the initial beamforming parameters are set with $\theta_{lm} = 0, \forall l, m$. And the association of terrestrial users and RISs are all generated randomly subject to (13c), (13d) and (13e) at the beginning.

Fig. 3 illustrates the total transmit power of all the UAVs versus the number of terrestrial users U whose data transmission and illumination requirement are satisfied by UAVs. Scheme I and Scheme II represent the proposed iterative algorithm with RISs' association optimized by dual method and greedy algorithm, respectively. And the initial scheme represents the scheme with initial settings. In global optimal scheme, we randomly set multiple initial points and choose the one that gets to the minimum transmit power as the global optimal solution. As can be seen, our proposed two schemes both work well compared with other schemes. Particularly, Scheme I outperforms Scheme II due to the fact that greedy algorithm searches a local optimal solution at each step while the dual method can find the global optimal solution when optimizing RISs association. Although the global optimal scheme can achieve the best performance, the gaps between the proposed schemes and the global optimal scheme are small, which indicates that the proposed schemes approach the optimal solution. Meanwhile, the total transmit power increases with the number of terrestrial users increasing. This is because the UAVs have to satisfy the demand of all the terrestrial users including the newcome terrestrial users. In addition, the schemes that only optimize one of these four optimization variables are also shown in Fig. 3. It is obvious that these four schemes all have the ability to reduce the total transmit power of UAVs. And the scheme that only optimizes the user association outperforms the other three schemes. This implies that the total transmit power can be constructively reduced with an appropriate user association. And it is reasonable to only optimize user association when requiring an urgent deployment. Moreover, we can find that

This article has been accepted for publication in a future issue of this journal, but has not been fully edited. Content may change prior to final publication. Citation information: DOI 10.1109/TWC.2022.3165853, IEEE Transactions on Wireless Communications

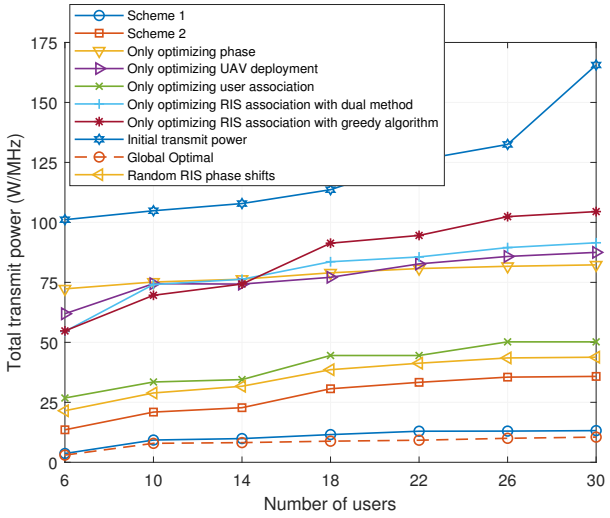

Fig. 3: Total transmit power versus number of users U.

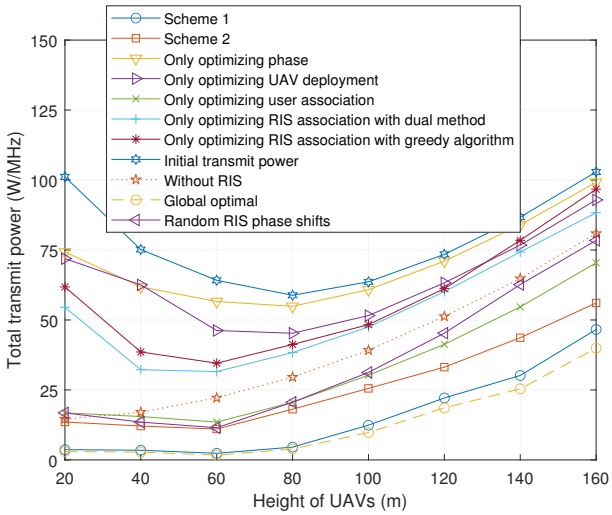

Fig. 4: Total transmit power versus height of UAVs H.

there is a plateau when the number of users growths from 10 to 14. This may be explained by that the power needs to be provided for the newcome users is less than the power needed by the user who requires the most transmit power in the same aerial area.

Fig. 4 shows that the total transmit power versus the height of UAVs H. It is interesting to find that the power required by the two proposed schemes decreases before it increases. And when the height is around 60m, the total transmit power achieves the minimum value. In order to find out the reasons behind this phenomenon, we also plot a dotted-line that reflects the changes of transmit power as the UAVs fly higher when no RISs deployed. We can see that this line increases monotonously, which indicates that the existence of the UAV-RIS-user link makes the total channel gain increases first and turn to decrease later as the increase of the height of UAVs. This is due to in large part the fact that when the UAVs fly from 20m to 60m, the value of cosine of emission angles gets larger. And the impact of the increase of emission angles on the total transmit power is greater than that of the increase of UAVs' height. However, when the height of UAVs grows more than 60m, the impact of the increase of the height is greater than that of the increase of emission angles. When there exists no RISs, only the height of UAVs has an influence on the total transmit power of all the UAVs. Hence, in this case, transmit power will always increase as the height increases. Furthermore, the four schemes that optimizes part of the variables all emerge similar trends as the proposed two schemes and global optimal scheme, which can also be attributed to the UAV-RIS-user links. The random RIS phase shifts scheme outperforms scheme without RISs, which can be explained by that the RISs can establish new links, thus the signals received at the terrestrial users are strengthened. Moreover, the scheme that only optimizes user association is least affected as the height rises from 20m to 60m. This is due to the fact that by allocating terrestrial users to a closer UAV, the emission angles of UAVs get smaller, thus the impact of the changes of angles gets reduced. As a comparison, the total power of the scheme that only optimizes phases, where the locations of UAVs, RISs association and users association all keep fixed, does not increase until 80m.

Fig. 5 depicts how the total transmit power of UAVs to meet the traffic rate and illumination requirement of all the terrestrial users changes as the number of RISs L varies. As can be seen, with the number of RISs increasing in this specific area, the transmit power of all the schemes decreases. Since a RIS, of which the phase of each reflective elements is optimized, can greatly improve the channel state between a UAV and its associated terrestrial users, the total transmit power will decrease correspondingly as the number of RISs increases. Adding one RIS with $M = 5$ reflective elements yields up to 23.01% and 18.58% reductions with respect to the total transmit power on average through Scheme I and Scheme II, respectively. In addition, even though we do not optimize any variables, the total transmit power can still reduce by 21.73% on average with initial all the phases equal to zero each time that a RIS is added randomly. This can be explained by that the increased RISs can establish new links, thus strengthening the signals received at the terrestrial users. Furthermore, the gap between our proposed algorithm and the global optimal solution reduces as the number of reflective elements of each RIS increases. In practical scenario, the number of reflective elements is large in each RIS. Therefore, our proposed algorithm can achieve a relatively high power efficiency with a low computational complexity.

Fig. 6 illustrates the total transmit power versus the number of reflective elements of each RIS M with 6 users and 10 users, respectively. As can be seen, the transmit power decreases with the number of reflective elements increasing, which is similar to what is shown in Fig. 5. And the proposed Scheme I outperforms Scheme II in terms to the total power. Meanwhile, both Scheme I and Scheme II outperform the scheme without RISs by up to 29.56% and 22.79% in the aspects of total transmitting power, respectively, when the number of terrestrial users is 6. When there are 10 terrestrial users, the performance of Scheme I and Scheme II yields up to 34.85% and 32.11% improvement, respectively. According

This article has been accepted for publication in a future issue of this journal, but has not been fully edited. Content may change prior to final publication. Citation information: DOI 10.1109/TWC.2022.3165853, IEEE Transactions on Wireless Communications

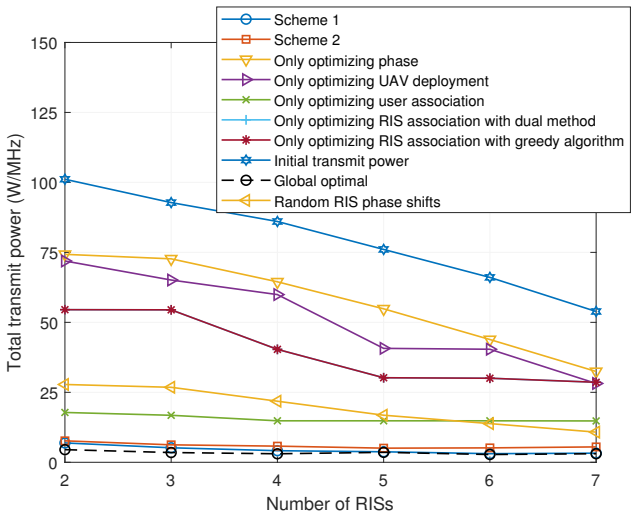

Fig. 5: Total transmit power versus number of RISs L.

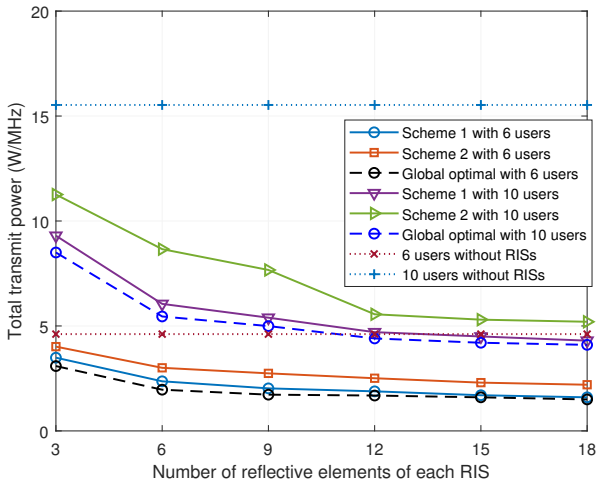

Fig. 6: Total transmit power versus number of reflective elements of each RIS M.

to Fig. 5 and Fig. 6, we can find out that increasing the number of either RISs or reflective elements of each RIS can constructively reduce the total transmit power.

To further evaluate the computational efficiency of the two proposed schemes, Table II displays the running time of the two schemes in an iteration on average when the numbers of terrestrial users are 9 and 15, respectively. It can be seen that Scheme I needs more time than Scheme II. This is caused by the fact that Scheme I searches for a global minimum point through multiple iterations when optimizing RISs association, while Scheme II only optimizes one RISs at one time until all the RISs' associations are optimized. However, from Fig. 3-6, we can find that Scheme I outperforms Scheme II in terms to total transmit power performance. In summary, the deployment optimized by Scheme I has better power performance, which are suitable for effective communication. While Scheme II is preferable for urgent communication due to its less running time.

TABLE II: Running Time of Two Schemes in an Iteration on Average

Number of users	Scheme I	Scheme II
9	4.64s	3.99s
15	11.237s	5.02s

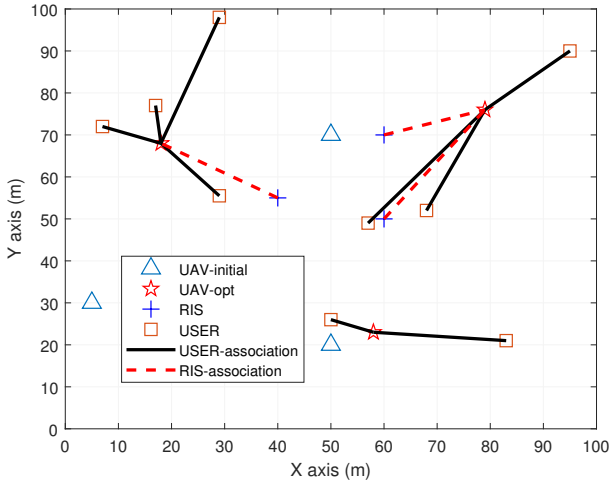

Fig. 7: One example of Scheme I.

Fig. 7 and Fig. 8 show two illustrative examples of the proposed Scheme I where the initial parameters are set randomly. In these two figures, the initial and the optimal locations of UAVs are denoted by triangles and pentacles, respectively. As can be seen, the optimal locations of UAVs are surrounded by its associated users and RISs. Furthermore, a small number of users who are distant from most users are served by an individual UAV, which can reduce the total transmit power significantly. In Fig. 8, however, one UAV is idle. This is because, during the period of optimization, the users who are originally associated with this UAV lead to less total power if they are served by the other UAVs. What can be predicted is that when terrestrial users are close enough to each other, maybe one UAV is enough. Moreover, as can be seen from Fig. 7 and Fig. 8, each RIS is associated with the closest UAV among all the UAVs. This can be explained by that short distance between UAV and RIS can enhance the channel gains between UAV and terrestrial users, thus reducing the transmit power.

V. CONCLUSION

In this paper, we proposed a novel framework of a VLC-enabled UAV multi-cell network, by leveraging the prevalent RISs for reducing total consuming power of all the UAVs. An optimization problem was formulated to dynamically optimize UAV deployment, RISs phase shift, users and RISs association to achieve the minimum total transmitting power by taking into account traffic and illumination demands. An alternating algorithm was proposed to solve multiple subproblems iteratively. Numerical results show the superior performance of our proposed algorithms over the case without RIS with respect to energy consumption reduction. And by associating each RIS

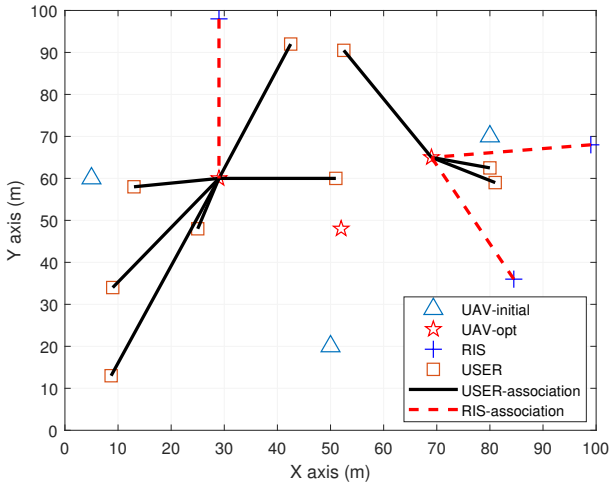

Fig. 8: The other example of Scheme I.

with the closest UAV, we can achieve the minimum transmit power of all the UAVs. In future work, we will further investigate UAVs' height optimization problem for more practical scenario with obstacles. In this case, the employment of UAVs should be carefully designed. We will also consider robust design for UAV assisted VLC systems. Moreover, we will extend our work to satellite communications. We also expect to design an algorithm for RISs' locations optimization in the future.

REFERENCES

[1] C. Kai, H. Li, L. Xu, Y. Li, and T. Jiang, "Energy-efficient device-to-device communications for green smart cities," *IEEE Transactions on Industrial Informatics*, vol. 14, no. 4, pp. 1542–1551, Jan. 2018.

[2] X. Chen, L. Pu, L. Gao, W. Wu, and D. Wu, "Exploiting massive D2D collaboration for energy-efficient mobile edge computing," *IEEE Wireless Communications*, vol. 24, no. 4, pp. 64–71, Aug. 2017.

[3] Y. Hu, M. Chen, W. Saad, H. V. Poor, and S. Cui, "Distributed multi-agent meta learning for trajectory design in wireless drone networks," *IEEE Journal on Selected Areas in Communications*, vol. 39, no. 10, pp. 3177–3192, Oct. 2021.

[4] S. Hu, W. Ni, X. Wang, A. Jamalipour, and D. Ta, "Joint optimization of trajectory, propulsion, and thrust powers for covert uav-on-uav video tracking and surveillance," *IEEE Transactions on Information Forensics and Security*, vol. 16, pp. 1959–1972, Dec. 2021.

[5] S. Hu, Q. Wu, and X. Wang, "Energy management and trajectory optimization for uav-enabled legitimate monitoring systems," *IEEE Transactions on Wireless Communications*, vol. 20, no. 1, pp. 142–155, Sep. 2021.

[6] F. Tariq, M. R. A. Khandaker, K. K. Wong, M. A. Imran, M. Bennis, and M. Debbah, "A speculative study on 6G," *IEEE Wireless Communications*, vol. 27, no. 4, pp. 118–125, Aug. 2020.

[7] M. Chen, Z. Yang, W. Saad, C. Yin, H. V. Poor, and S. Cui, "A joint learning and communications framework for federated learning over wireless networks," *IEEE Transactions on Wireless Communications*, vol. 20, no. 1, pp. 269–283, 2021.

[8] S. Hu, X. Chen, W. Ni, E. Hossain, and X. Wang, "Distributed machine learning for wireless communication networks: Techniques, architectures, and applications," *IEEE Communications Surveys Tutorials*, vol. 23, no. 3, pp. 1458–1493, June 2021.

[9] Q. Wu and R. Zhang, "Towards smart and reconfigurable environment: Intelligent reflecting surface aided wireless network," *IEEE Communications Magazine*, vol. 58, no. 1, pp. 106–112, Nov. 2020.

[10] C. Huang, A. Zappone, G. C. Alexandropoulos, M. Debbah, and C. Yuen, "Reconfigurable intelligent surfaces for energy efficiency in wireless communication," *IEEE Transactions on Wireless Communications*, vol. 18, no. 8, pp. 4157–4170, Aug. 2019.

[11] C. Huang, S. Hu, G. C. Alexandropoulos, A. Zappone, C. Yuen, R. Zhang, M. D. Renzo, and M. Debbah, "Holographic MIMO surfaces for 6G wireless networks: Opportunities, challenges, and trends," *IEEE Wireless Communications*, vol. 27, no. 5, pp. 118–125, Oct. 2020.

[12] C. Pan, H. Ren, K. Wang, J. F. Kolb, M. Elkashlan, M. Chen, M. Di Renzo, Y. Hao, J. Wang, A. L. Swindlehurst, X. You, and L. Hanzo, "Reconfigurable intelligent surfaces for 6G systems: Principles, applications, and research directions," *IEEE Communications Magazine*, vol. 59, no. 6, pp. 14–20, June 2021.

[13] C. Pan, H. Ren, K. Wang, W. Xu, M. Elkashlan, A. Nallanathan, and L. Hanzo, "Multicell MIMO communications relying on intelligent reflecting surfaces," *IEEE Transactions on Wireless Communications*, vol. 19, no. 8, pp. 5218–5233, May 2020.

[14] S. Zeng, H. Zhang, B. Di, Z. Han, and L. Song, "Reconfigurable intelligent surface (RIS) assisted wireless coverage extension: RIS orientation and location optimization," *IEEE Communications Letters*, vol. 25, no. 1, pp. 269–273, Sep. 2021.

[15] Z. Yang, W. Xu, C. Huang, J. Shi, and M. Shikh-Bahaei, "Beamforming design for multiuser transmission through reconfigurable intelligent surface," *IEEE Transactions on Communications*, vol. 69, no. 1, pp. 589–601, Jan. 2021.

[16] C. Huang, R. Mo, and C. Yuen, "Reconfigurable intelligent surface assisted multiuser MISO systems exploiting deep reinforcement learning," *IEEE Journal on Selected Areas in Communications*, vol. 38, no. 8, pp. 1839–1850, Aug. 2020.

[17] V. C. Thirumavalavan and T. S. Jayaraman, "BER analysis of reconfigurable intelligent surface assisted downlink power domain NOMA system," in *Proc. of International Conference on COMmunication Systems NETworkS (COMSNETS)*, Bengaluru, India, March 2020, pp. 519–522.

[18] L. Yang and Y. Yuan, "Secrecy outage probability analysis for RIS-assisted NOMA systems," *Electronics Letters*, vol. 56, no. 23, pp. 1254–1256, Nov. 2020.

[19] M. Elhattab, M. A. Arfaoui, C. Assi, and A. Ghrayeb, "Reconfigurable intelligent surface assisted coordinated multipoint in downlink NOMA networks," *IEEE Communications Letters*, vol. 25, no. 2, pp. 632–636, Feb. 2021.

[20] M. Zhang, M. Chen, Z. Yang, H. Asgari, and M. Shikh-Bahaei, "Joint user clustering and passive beamforming for downlink NOMA system with reconfigurable intelligent surface," in *Proc. of IEEE Annual International Symposium on Personal, Indoor and Mobile Radio Communications*, London, United Kingdom, United Kingdom, Oct. 2020, pp. 1–6.

[21] T. Hou, Y. Liu, Z. Song, X. Sun, Y. Chen, and L. Hanzo, "Reconfigurable intelligent surface aided NOMA networks," *IEEE Journal on Selected Areas in Communications*, vol. 38, no. 11, pp. 2575–2588, July 2020.

[22] Y. Xu, M. Chen, Z. Yang, Y. Liu, H. Long, and M. Shikh-Bahaei, "Fair non-orthogonal multiple access communication systems with reconfigurable intelligent surface," in *Proc. of IEEE Annual International Symposium on Personal, Indoor and Mobile Radio Communications*, London, United Kingdom, United Kingdom, Oct. 2020, pp. 1–6.

[23] Y. Li, M. Jiang, Q. Zhang, and J. Qin, "Joint beamforming design in multi-cluster MISO NOMA reconfigurable intelligent surface-aided downlink communication networks," *IEEE Transactions on Communications*, vol. 69, no. 1, pp. 664–674, Jan. 2021.

[24] M. Jian and Y. Zhao, "A modified off-grid SBL channel estimation and transmission strategy for RIS-assisted wireless communication systems," in *Proc. of International Wireless Communications and Mobile Computing (IWCMC)*, Limassol, Cyprus, July 2020, pp. 1848–1853.

[25] M. Nemati, J. Park, and J. Choi, "Ris-assisted coverage enhancement in millimeter-wave cellular networks," *IEEE Access*, vol. 8, pp. 188 171–188 185, Oct. 2020.

[26] X. Yang, C. K. Wen, and S. Jin, "MIMO detection for reconfigurable intelligent surface-assisted millimeter wave systems," *IEEE Journal on Selected Areas in Communications*, vol. 38, no. 8, pp. 1777–1792, June 2020.

[27] N. S. Perović, M. D. Renzo, and M. F. Flanagan, "Channel capacity optimization using reconfigurable intelligent surfaces in indoor mmWave environments," in *Proc. of ICC IEEE International Conference on Communications (ICC)*, Dublin, Ireland, July 2020, pp. 1–7.

[28] J. Zhang, Z. Zheng, Z. Fei, and X. Bao, "Positioning with dual reconfigurable intelligent surfaces in millimeter-wave MIMO systems," in *Proc. of International Conference on Communications in China (ICCC)*, Chongqing, China, Nov. 2020, pp. 800–805.

[29] L. Grobe, A. Paraskevopoulos, J. Hilt, D. Schulz, F. Lassak, F. Hartlieb, C. Kottke, V. Jungnickel, and K. Langer, "High-speed visible light communication systems," *IEEE Communications Magazine*, vol. 51, no. 12, pp. 60–66, Dec. 2013.

[30] S. Wu, H. Wang, and C. Youn, "Visible light communications for 5G wireless networking systems: from fixed to mobile communications," *IEEE Network*, vol. 28, no. 6, pp. 41–45, Nov. 2014.

[31] J. J. D. McKendry, D. Massoubre, S. Zhang, B. R. Rae, R. P. Green, E. Gu, R. K. Henderson, A. E. Kelly, and M. D. Dawson, "Visible-light communications using a CMOS-controlled micro-light- emitting-diode array," *Journal of Lightwave Technology*, vol. 30, no. 1, pp. 61–67, Nov. 2012.

[32] P. H. Pathak, X. Feng, P. Hu, and P. Mohapatra, "Visible light communication, networking, and sensing: A survey, potential and challenges," *IEEE Communications Surveys Tutorials*, vol. 17, no. 4, pp. 2047–2077, Sep. 2015.

[33] D. Karunatilaka, F. Zafar, V. Kalavally, and R. Parthiban, "LED based indoor visible light communications: State of the art," *IEEE Communications Surveys Tutorials*, vol. 17, no. 3, pp. 1649–1678, Mar. 2015.

[34] A. Amantayeva, M. Yerzhanova, and R. C. Kizilirmak, "UAV location optimization for UAV-to-Vehicle multiple access channel with visible light communication," in *Proc. of Wireless Days (WD)*, Manchester, UK, Apr. 2019, pp. 1–4.

[35] Y. Wang, M. Chen, Z. Yang, T. Luo, and W. Saad, "Deep learning for optimal deployment of UAVs with visible light communications," *IEEE Transactions on Wireless Communications*, vol. 19, no. 11, pp. 7049–7063, July 2020.

[36] Q. V. Pham, T. Huynh-The, M. Alazab, J. Zhao, and W. J. Hwang, "Sum-rate maximization for UAV-assisted visible light communications using NOMA: Swarm intelligence meets machine learning," *IEEE Internet of Things Journal*, vol. 7, no. 10, pp. 10 375–10 387, Apr. 2020.

[37] K. Lee, H. Park, and J. R. Barry, "Indoor channel characteristics for visible light communications," *IEEE Communications Letters*, vol. 15, no. 2, pp. 217–219, Jan. 2011.

[38] C. Huang and X. Zhang, "LOS-NLOS identification algorithm for indoor visible light positioning system," in *Proc. of International Symposium on Wireless Personal Multimedia Communications (WPMC)*, Bali, Indonesia, Dec. 2017, pp. 575–578.

[39] P. Wang, J. Fang, L. Dai, and H. Li, "Joint transceiver and large intelligent surface design for massive mimo mmwave systems," *IEEE Transactions on Wireless Communications*, vol. 20, no. 2, pp. 1052–1064, Feb. 2021.

[40] Z. Yang, M. Chen, W. Saad, W. Xu, M. Shikh-Bahaei, H. V. Poor, and S. Cui, "Energy-efficient wireless communications with distributed reconfigurable intelligent surfaces," *IEEE Transactions on Wireless Communications*, pp. 1–1, July 2021.

[41] Z. Yang, W. Xu, C. Huang, J. Shi, and M. Shikh-Bahaei, "Beamforming design for multiuser transmission through reconfigurable intelligent surface," *IEEE Transactions on Communications*, vol. 69, no. 1, pp. 589–601, Oct. 2021.

[42] A. Amantayeva, M. Yerzhanova, and R. C. Kizilirmak, "Uav location optimization for uav-to-vehicle multiple access channel with visible light communication," in *Proc. of Wireless Days (WD)*, Manchester, UK, April 2019, pp. 1–4.

[43] S. Li, B. Duo, X. Yuan, Y. Liang, and M. Di Renzo, "Reconfigurable intelligent surface assisted UAV communication: Joint trajectory design and passive beamforming," *IEEE Wireless Communications Letters*, vol. 9, no. 5, pp. 716–720, Jan. 2020.

[44] Q. Wu and R. Zhang, "Intelligent reflecting surface enhanced wireless network via joint active and passive beamforming," *IEEE Transactions on Wireless Communications*, vol. 18, no. 11, pp. 5394–5409, Nov. 2019.

[45] Z.-q. Luo, W.-k. Ma, A. M.-c. So, Y. Ye, and S. Zhang, "Semidefinite relaxation of quadratic optimization problems," *IEEE Signal Processing Magazine*, vol. 27, no. 3, pp. 20–34, April 2010.

Yihan Cang (Student Member, IEEE) received the B.S. degree in communication engineering from Nanjing University of Posts and Telecommunications, Nanjing, China, in 2019. He is currently working towards his Ph.D. degree in information and communications engineering with National Mobile Communications Research Laboratory, Southeast University, Nanjing, China. His research interests include multi-access edge computing, visible light communications, and resource allocation in communications.

Ming Chen (Member, IEEE) received his Ph.D. degrees from mathematics department of Nanjing University, Nanjing, China, in 1996. In July of 1996, he came to National Mobile Communications Research Laboratory of Southeast University in Nanjing to be a Lecturer. From 1998 to 2003 he has been an Associate Professor and from 2003 to now a professor at the laboratory. His research interests include baseband signal processing, radio and computing resource allocation and network planning for all generation mobile communication systems, visible light communication systems, mobile edge computing systems and satellite mobile communications. He has completed more than 40 research projects in the role of director by now, among which there are more than 15 projects are issued by national ministries, supervised more than 30 Ph. D. and 100 M. Sc. Students and published more than 300 journal papers as coauthor. He won twice the first level provincial progress awards in science and technology.

Jingwen Zhao (Student Member, IEEE) received the B.S. degree in electronic information engineering from Zhengzhou University, Zhengzhou, China, in 2019. She is currently pursuing the Ph.D. degree with National Mobile Communications Research Laboratory, Southeast University, Nanjing, China. Her research interests mainly include mobile edge computing, intelligent reflection surface, UAV communication, wireless communications, and visible light communications.

Zhaohui Yang (Member, IEEE) (S'14-M'18) received the B.S. degree in information science and engineering from Chien-Shiung Wu Honors College, Southeast University, Nanjing, China, in June 2014, and the Ph.D. degree in communication and information system with the National Mobile Communications Research Laboratory, Southeast University, Nanjing, China, in May 2018. From May 2018 to October 2020, he was a postdoctoral research associate with the Center for Telecommunications Research, Department of Informatics, King's College London, UK. He is currently a visiting associate professor with College of Information Science and Electronic Engineering Zhejiang Key Lab of Information Processing Communication and Networking, Zhejiang University, and also a research fellow with the Department of Electronic and Electrical Engineering, University College London, UK. He is an Associate Editor for the IEEE Communications Letters, IET Communications and EURASIP Journal on Wireless Communications and Networking. He has guest edited a feature topic of IEEE Communications Magazine on Communication Technologies for Efficient Edge Learning and a special issue of Journal on Selected Areas in Communications for Beyond Transmitting Bits: Context, Semantics and Task-Oriented Communications. He was a Co-Chair for workshops on edge learning and wireless communications in several conferences including the IEEE International Conference on Communications (ICC), the IEEE Global Telecommunication Conference (GLOBECOM), the IEEE Wireless Communications and Networking Conference (WCNC), and the IEEE International Symposium on Personal, Indoor and Mobile Radio Communication (PIMRC). His research interests include federated learning, reconfigurable intelligent surface, UAV, and NOMA. He was a TPC member of IEEE ICC during 2015-2021 and GLOBECOM during 2017-2021. He was an exemplary reviewer for IEEE Transactions on Communications in 2019 and 2020.

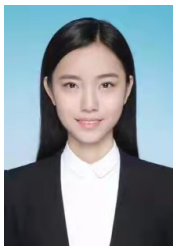

Ye Hu (Member, IEEE) (S'17) received her PhD. in the Bradley department of Electrical and Computer Engineering at Virginia Tech, Virginia, USA, in 2021, and her M.S. in Information and Communication Engineering Department, Beijing University of Posts and Telecommunications, Beijing, China, in 2017. She is now a postdoctoral research scientist at the Electrical Engineering Department at Columbia University, New York, USA. Her research interests include machine leaning, game theory, cyber-physical systems, cybersecurity, unmanned aerial vehicles, and wireless communication. She was also the author of the best paper award at IEEE GLOBECOM in 2020.

Chongwen Huang (Member, IEEE) obtained his B. Sc. degree in 2010 from Nankai University, and the M.Sc degree from the University of Electronic Science and Technology of China in 2013, and PhD degree from Singapore University of Technology and Design (SUTD) in 2019. From Oct. 2019 to Sep. 2020, He is a Postdoc in SUTD. Since Sep. 2020, he joined into Zhejiang University as a tenure-track young professor. Dr. Huang is the recipient of IEEE Marconi Prize Paper Award in Wireless Communications, and IEEE ComSoc Asia-Pacific Outstanding Young Researcher Award in 2021. He has served as an Editor of IEEE Communications Letter, Elsevier Signal Processing, EURASIP Journal on Wireless Communications and Networking and Physical Communication since 2021. His main research interests are focused on Holographic MIMO Surface/Reconfigurable Intelligent Surface, B5G/6G Wireless Communication, mmWave/THz Communications, Deep Learning technologies for Wireless communications, etc.

Kai-Kit Wong (Fellow, IEEE) (M'01-SM'08-F'16) received the BEng, the MPhil, and the PhD degrees, all in Electrical and Electronic Engineering, from the Hong Kong University of Science and Technology, Hong Kong, in 1996, 1998, and 2001, respectively. After graduation, he took up academic and research positions at the University of Hong Kong, Lucent Technologies, Bell-Labs, Holmdel, the Smart Antennas Research Group of Stanford University, and the University of Hull, UK. He is Chair in Wireless Communications at the Department of Electronic and Electrical Engineering, University College London, UK. His current research centers around 5G and beyond mobile communications. He is a co-recipient of the 2013 IEEE Signal Processing Letters Best Paper Award and the 2000 IEEE VTS Japan Chapter Award at the IEEE Vehicular Technology Conference in Japan in 2000, and a few other international best paper awards. He is Fellow of IEEE and IET and is also on the editorial board of several international journals. He is the Editor-in-Chief for IEEE Wireless Communications Letters since 2020.